

Photochemical and Photoelectrochemical Reduction of CO₂

Bhupendra Kumar,¹ Mark Llorente,¹ Jesse Froehlich,²
Tram Dang,¹ Aaron Sathrum,¹
and Clifford P. Kubiak^{1,2}

¹Materials Science and Engineering Program, and ²Department of Chemistry and Biochemistry, University of California, San Diego, La Jolla, California 92093; email: ckubiak@ucsd.edu

Annu. Rev. Phys. Chem. 2012. 63:541–69

First published online as a Review in Advance on
January 30, 2012

The *Annual Review of Physical Chemistry* is online at
physchem.annualreviews.org

This article's doi:
10.1146/annurev-physchem-032511-143759

Copyright © 2012 by Annual Reviews.
All rights reserved

0066-426X/12/0505-0541\$20.00

Keywords

solar fuels, molecular catalyst, photocathode, semiconductor/catalyst junction, homogeneous catalysis, heterogeneous catalysis

Abstract

The recent literature on photochemical and photoelectrochemical reductions of CO₂ is reviewed. The different methods of achieving light absorption, electron-hole separation, and electrochemical reduction of CO₂ are considered. Energy gap matching for reduction of CO₂ to different products, including CO, formic acid, and methanol, is used to identify the most promising systems. Different approaches to lowering overpotentials and achieving high chemical selectivities by employing catalysts are described and compared.

1. INTRODUCTION

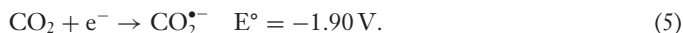
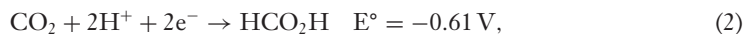
1.1. General Introduction

Research in the field of photochemical and photoelectrochemical reduction of CO₂ has grown rapidly in the last few decades. This growing research effort is a response by physical scientists and engineers to the increasing amount of CO₂ in the atmosphere and the steady growth in global fuel demand. This review presents much of the significant work done in this field over the past three decades. It then extends the discussion to a critical summary of previous work and prospects for future directions to develop catalytic systems that will reduce CO₂ with high efficiencies.

The catalytic conversion of CO₂ to liquid fuels is a critical goal that would positively impact the global carbon balance by recycling CO₂ into usable fuels. The challenges presented here are great, but the potential rewards are enormous. CO₂ is an extremely stable molecule generally produced by fossil fuel combustion and respiration. Returning CO₂ to a useful state by activation/reduction is a scientifically challenging problem, requiring appropriate catalysts and energy input. This poses several fundamental challenges in chemical catalysis, electrochemistry, photochemistry, and semiconductor physics and engineering.

1.2. The Difficulty of CO₂ Reduction

The thermodynamic potentials for various CO₂ reduction products can be seen in Equations 1–5 (pH 7 in aqueous solution versus a normal hydrogen electrode (NHE), 25°C, 1 atm gas pressure, and 1 M for other solutes) (1):



Although CO₂ has been shown to be reduced directly on metal surfaces, the overpotentials are either exceedingly high or the metal surfaces become poisoned and deactivated by the reduction products (2). In addition to thermodynamic considerations, there are also considerable kinetic challenges to the conversion of CO₂ to more complex products. Typically, multiple proton-coupled electron transfer (PCET) steps must be orchestrated with their own associated activation energies presenting kinetic barriers to the forward reaction. A great deal of success has been achieved in the reduction of CO₂ to CO and formate. However, the multiple electron and proton transfers necessary to produce more useful products such as methane or methanol have only been demonstrated with low efficiency. To achieve success at efficient production of a CO₂ reduction product that can serve as a liquid fuel directly (i.e., methanol) would be a considerable milestone for renewable energy and energy storage research.

1.3. Molecular Catalysts

To overcome the thermodynamic barriers of CO₂ reduction, molecular catalysts can be used to lower the overpotential by stabilizing the intermediate transition states between the linear CO₂ molecules and the intended product. CO₂ has multiple known binding modes to transition metal complexes (3). The metal can then act as an inner sphere electron transfer agent to activate CO₂ for

further transformation. With the choice of various metal centers and ligand structures, molecular catalysts are highly tunable to achieve intended properties such as fast kinetics and long-term stability. The performance of a molecular catalyst can be judged by the following figures of merit:

$$\text{Faradaic efficiency (FE)} = (\text{moles product/moles of electrons passed}) \\ \times (\text{number of electrons needed for conversion}),$$

$$\text{Overpotential} = \text{applied potential at a given current density} \\ - \text{thermodynamic potential for conversion.}$$

$$\text{Turnover number (TON)} = \text{moles intended products/moles catalyst},$$

$$\text{Catalytic selectivity (CS)} = \text{moles intended products}/(\text{moles H}_2 + \text{moles other products}),$$

$$\text{Turnover frequency (TOF)} = \text{catalytic turnovers per unit time.}$$

Further information regarding molecular catalysts for CO₂ reduction can be found in recently published reviews (1, 4).

1.4. Photochemical and Photoelectrochemical Reduction of CO₂

There are several ways to reduce CO₂ with the assistance of renewable solar energy, and these methods can be divided into three major categories: homogeneous photoreduction by a molecular catalyst, photoelectrochemical reduction by a semiconducting photocathode, and electrochemical reduction by an electrolyzer powered by commercial photovoltaic (PV) devices.


A homogeneous CO₂ photoreduction system consists of a molecular catalyst, light absorber, sacrificial electron donor, and/or electron relay. When looking at these types of systems, the main figure of merit is the photochemical quantum yield, defined as

$$\text{Photochemical quantum yield } (\Phi) = (\text{moles products/absorbed photons}) \\ \times (\text{number of electrons needed for conversion}).$$

In a heterogeneous system, p-type semiconductor/liquid junctions are extensively studied as PV devices. The p-type semiconducting electrodes can act as photocathodes for photoassisted CO₂ reduction. **Figure 1** shows four different schemes of photoassisted reduction of CO₂ using a semiconducting photocathode: (a) direct heterogeneous CO₂ reduction by a biased semiconductor photocathode (5–26), (b) heterogeneous CO₂ reduction by metal particles on a biased semiconductor photocathode (6, 13, 15, 27–35), (c) homogeneous CO₂ reduction by a molecular catalyst through a semiconductor/molecular catalyst junction (36–43), and (d) heterogeneous CO₂ reduction by a molecular catalyst attached to the semiconductor photocathode surface (13, 22, 44–46).

There are several examples where PV-powered commercial electrolyzers have been used for hydrogen generation (47–49), but very few of these setups exist for CO₂ reduction to an energy-dense product (50–53). The idea to power an electrolyzer by a PV device was first proposed by Bard & Fox (54) for the water splitting electrolyzer. Recently, Delacourt et al. (55) reported a PV-powered electrolyzer that forms syngas (CO and H₂) from CO₂ and water.

For these different systems, the expressions for solar to chemical energy conversion efficiency are complicated because multiple products can form at the cathode and anode. In most cases, CO₂ photoelectrochemical reduction on photocathodes happens at high overpotentials, which further complicates this calculation. A detailed description of the different efficiency expressions for CO₂ photoelectrochemical reduction is provided in **Supplemental Section 1** (follow the **Supplemental Material** link from the Annual Reviews home page at <http://www.annualreviews.org>). These

 **Supplemental Material**

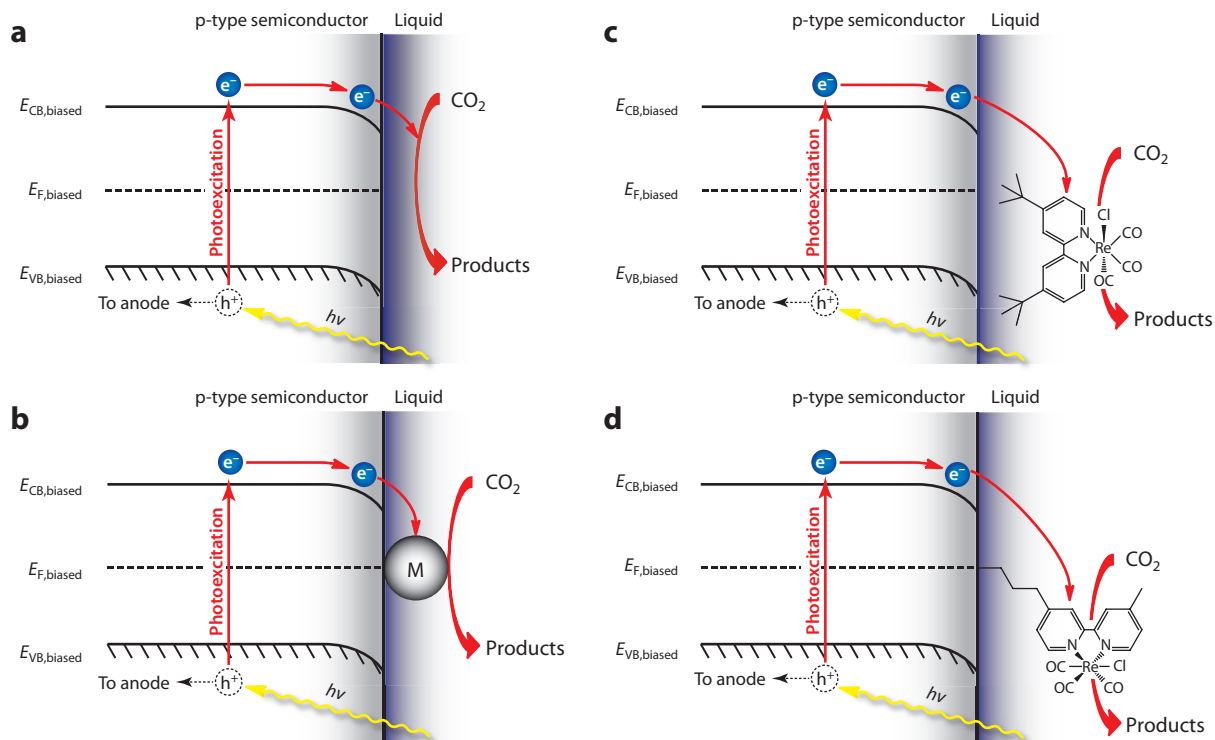


Figure 1

Schematic diagrams of four different schemes for light-assisted CO₂ reduction on a semiconducting photocathode:

(a) heterogeneous catalysis on a semiconductor electrode, (b) heterogeneous catalysis on a metal-decorated semiconductor electrode, (c) homogeneous catalysis through a semiconductor/molecular catalyst junction, and (d) heterogeneous catalysis through a molecular catalyst-decorated semiconductor electrode.

supplemental equations can be used to calculate the efficiency for the following cell configurations: (a) a three-electrode cathodic half-cell reaction (**Supplemental Equations 1.1–1.3**), (b) a two-electrode photoelectrochemical cell (PEC) (**Supplemental Equation 1.4**), and (c) a two-electrode PV-powered electrolyzer (**Supplemental Equation 1.5**).

2. HOMOGENEOUS PHOTOCATALYTIC REDUCTION OF CO₂ WITH PHOTOSENSITIZER AND CATALYSTS

The generic mechanism of the photocatalytic reduction of CO₂ (Equations 6a–d, below) consists of a photosensitizer (P) capable of absorbing radiation in the ultraviolet or visible region and of the generation of an excited state (P^{*}). The excited state is reductively quenched by a sacrificial donor (D) generating a singly reduced photosensitizer (P[−]) and oxidized donor (D⁺). The choice of photosensitizer must be such that P[−] is able to transfer an electron efficiently to the catalyst species (cat) to generate the reduced catalyst species (cat[−]). In some cases the photosensitizer and the catalyst are the same species. The cat[−] is then able to bind CO₂ and proceed with the catalytic mechanism to release the intended products and regenerate cat. Common photosensitizers used in these systems include aromatics, e.g., p-terphenyl and phenazine, and polypyridine-coordinated transition metal complexes. Ruthenium(II) trisbipyridine ([Ru(bipy)₃]²⁺) is the most often

employed transition metal complex due to its strong visible-light absorption and high photostability (56). The most common catalyst species include macrocycle complexes of Ni and Co, polypyridine Ru and Re catalysts, and suspended metal colloids. The macrocycle and polypyridine complexes are the most efficient and therefore the focus of this section. There have been several excellent reviews on this subject that can be referred to for further details (57–59).



Conjugated metallomacrocycles such as corrins (60), corroles (61), porphyrins (61), and phthalocyanines (62) with a Co or Fe center have been shown to act as photocatalysts for CO₂ reduction. Such metallomacrocycles strongly absorb visible light and do not require the addition of a photosensitizer. These systems do, however, suffer from low Φ and low CS due to significant production of H₂. Tetraazamacrocyclics such as Ni(cyclam) have proved to reduce CO₂ efficiently and selectively to CO electrocatalytically while adsorbed on an Hg electrode (40). In purely photocatalytic systems, however, they tend to suffer from low Φ , CS, and TON (63, 64). When Co is used as the metal center, the photocatalytic properties are improved. In one early report, a series of cobalt tetraazamacrocycles was shown to photocatalyze the reduction of CO₂ using Ru(bipy)₃ as a photosensitizer and ascorbic acid as the sacrificial donor (65). This system displayed a reasonably high TON of 532 at very low catalyst concentrations (3.2 μM) but had poor selectivity (CS < 1) with H₂ cogeneration. Solutions of Co(III)cyclam with p-terphenyl as a photosensitizer and triethanolamine as sacrificial donors produced CO and formate as the major products, with quantum yields of 0.15 and 0.10, respectively (66). The reduction potential of the p-terphenyl radical anion is high enough to access the Co(I) state. Co(I) can then either bind CO₂ to form a Co-CO₂ adduct, which can then be protonated and reduced to produce CO and OH[−], or it can react with a proton to generate a hydride to which CO₂ can insert to form a Co-OOCH intermediate that will then release formate upon a second reduction (**Figure 2**). The identity of the amine sacrificial donor was shown to have an effect on the product distribution because it may also act as a ligand during the catalytic cycle. Formate was produced with much higher selectivity when phenazine was used as the photosensitizer because it was shown to function as an electron and hydrogen transfer agent (67).

A well-studied catalyst, Re(bipy)(CO)₃X (where bipy = 2,2'-bipyridine and X = Cl, Br), capable of selective production of CO without the use of a separate photosensitizer was developed by Lehn and coworkers (68, 69). ¹³CO was detected when using labeled ¹³CO₂, confirming that the CO originated from the photochemical reduction of CO₂. Under these conditions, however, complete exchange to the fully labeled complex Re(bipy)(¹³CO)₃Cl was also observed. The proposed catalytic cycle (**Figure 3**) demands an empty coordination site for CO₂ binding. Indeed, under illumination and in the presence of an electron donor, anion exchange of Cl[−] with Br[−] occurred, indicating that loss of halide could be generating the open coordination site. Adding excess X[−] ligand was shown to increase efficiency and stabilize CO production by inhibiting a competing mechanism in which halide loss, formation of a Re hydride, and CO₂ insertion leads to the formate complex, Re(bipy)CO₃(HCOO) (69). With the addition of phosphate groups to the Re(bipy)(CO)₃X system (X = P(OEt)₃), one of the highest single-molecule quantum efficiencies was reported for a homogeneous photocatalytic system (Φ = 0.38) (70). In a two-molecule system consisting of a 25:1 mixture of Re(bipy)(CO)₃P(OMe)₃ as photosensitizer and Re(bipy)(CO)₃MeCN as catalyst, even higher quantum yields were achieved (Φ = 0.59) (71). Triethanolamine was used

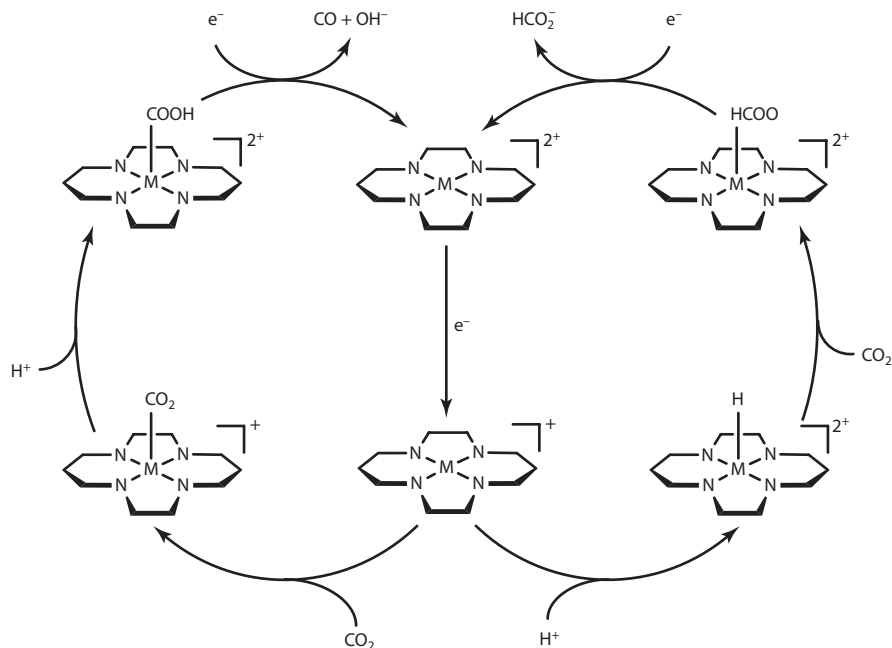


Figure 2

Proposed mechanism for CO and formate production from photocatalyzed reduction of CO₂ by tetraazamacrocyclic transition metal complexes (M = Co, Ni).

as a sacrificial donor. The MeCN ligand on the [Re(bipy)(CO)₃MeCN]⁺ complex is labile and easily generates an open CO₂ binding site. The [Re(bipy)(CO)₃(P(OMe)₃)]⁺ was chosen as the photosensitizer due to its efficient conversion to the reduced species.

Although the Re catalyst systems mentioned above demonstrated remarkable Φ , they lacked extended absorption in the visible region. For practical purposes, such as utilization of solar photons, absorption in the visible is desired. Ishitani and coworkers (72) have addressed this issue by utilizing a bridging ligand to covalently attach a [Ru(bipy)₃]²⁺-type photosensitizer, which absorbs strongly in the visible, to a Re(bipy)(CO)₃X type catalyst to create a supramolecular dyad complex. This dyad exhibited significantly better performances (Φ = 0.12, TON = 170) relative to a simple, noncovalently linked mixture of the photosensitizer and catalyst (Φ = 0.062, TON = 101), which the authors ascribe to more efficient intramolecular electron transfer from the reductively quenched Ru(bipy)₃-type species to the Re(bipy)(CO)₃X as compared with the intermolecular electron transfer that occurs for the mixture system. A subsequent publication reported the effect of the bridging ligand on the performance of the supramolecular catalyst: A Φ of 0.21 was achieved, which was the best reported value in homogeneous photocatalytic systems using low energy visible light > 500 nm (73).

Although the systems described above primarily produced CO as a CO₂ reduction product, it is worth noting that several systems selectively produce formate using Ru(bipy)₂XY (X = Y = CO) (74) (X = CO, Y = H) (75) in conjunction with Ru(bipy)₃ as the photosensitizer. The product formation was shown to be dependent on the presence of water and the identity of the sacrificial electron donor (74). A recent publication has examined the pathway for formate production using density functional theory (DFT) on a Re(bipy)(CO)₃Cl catalyst with triethylamine (TEA) as the

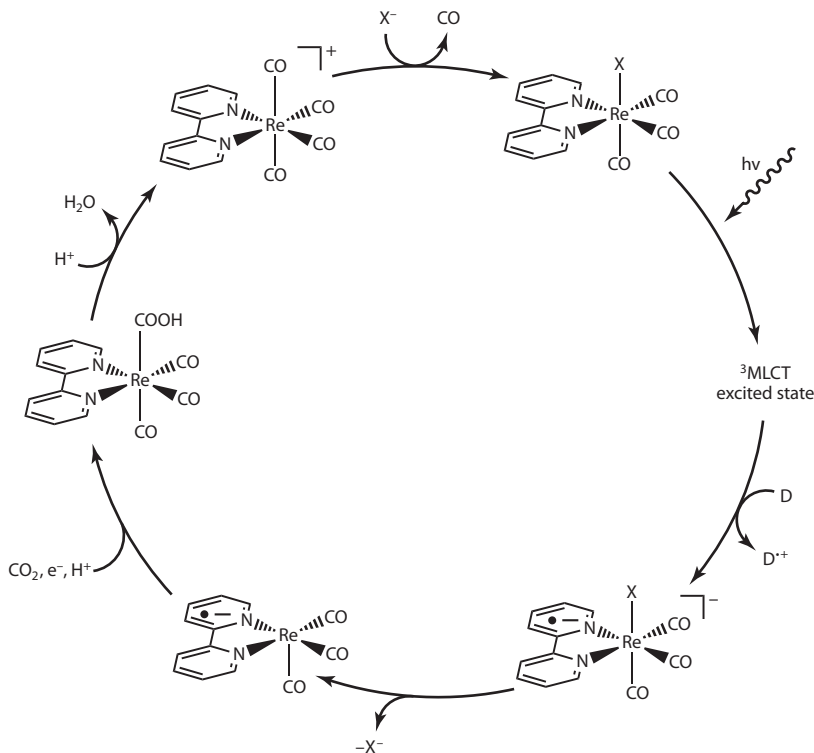


Figure 3

Proposed photocatalytic mechanism for CO production from a $\text{Re}(\text{bipy})(\text{CO})_3\text{X}$ catalyst. Abbreviation: MLCT, metal-to-ligand charge transfer.

sacrificial donor (76). The net catalytic cycle for formate production was predicted to be exothermic by 36.4 kcal/mol.

Although photocatalytic reduction of CO_2 may become an important stepping stone to solar fuel production, much progress remains before it becomes practical as an industrial process. Presently, TONs remain in the hundreds and TOFs are typically in the tens per hour. More mechanistic work must be done in order to understand and increase the stability and rates of these systems. These quantitative measures of catalytic systems must also be scrutinized because they are dependent on catalyst concentration and can vary drastically depending on the concentrations and volumes chosen for the experiment. TON can be especially misinterpreted because it is often not reported whether the catalytic activity stopped at the given TON or if the experiment was simply ended after a given time. To compound the problem, different solvents, electron donors, photosensitizers, and light sources are employed by the various groups studying these photocatalysts. A more uniform system of measure may be needed in order to fairly compare these catalyst systems.

Looking forward to improved systems with a more practical utility, we must consider some additional issues. Since many of the photocatalysts presently studied are metal complexes employing rare and expensive transition metals, it is especially important to raise the catalytic rate and long-term stability to make this process economically feasible. More work must be done using earth-abundant elements that could support large-scale undertakings such as solar fuel production.

Another drawback to the reviewed systems is the use of a sacrificial donor to supply the electrons for the reduction process. Ideally, water would be the source of both the electrons and hydrogen atoms for CO₂ reduction catalysis in an artificial photosynthetic process. These issues are not trivial and will take considerable effort and creativity to solve.

3. HETEROGENEOUS PHOTOELECTROCHEMICAL REDUCTION OF CO₂ ON SEMICONDUCTOR PHOTOCATHODES

Heterogeneous photoelectrochemical reduction of CO₂ on semiconductor surfaces has been explored extensively in the last three decades. **Figure 4** shows band edge positions versus an NHE for several common p- and n-type semiconductor electrodes with CO₂ reduction potentials for different products at pH = 1. The single-electron reduction of CO₂ to CO₂^{•-} is above the conduction band of most of the semiconductors shown in the figure. Thermodynamically, proton-assisted multielectron reduction potentials for CO₂ lie within the band gap of several semiconductors. However, kinetic limitations lead to high overpotential for electrochemical reduction of CO₂ on semiconductor photocathodes or dark cathodes, as tabulated in **Supplemental Table 1**.

Both aqueous (5, 6, 8, 11, 14–16, 22, 25–28, 34, 42, 91, 92) and nonaqueous (7, 10, 12, 13, 17–20, 23, 24, 29, 31–33) solvents have been used for direct CO₂ photoelectrochemical reduction on flat semiconductor surfaces, with the most commonly reported nonaqueous solvents being polypropylene carbonate, acetonitrile, dimethylformamide (DMF), dimethyl sulfoxide (DMSO), and

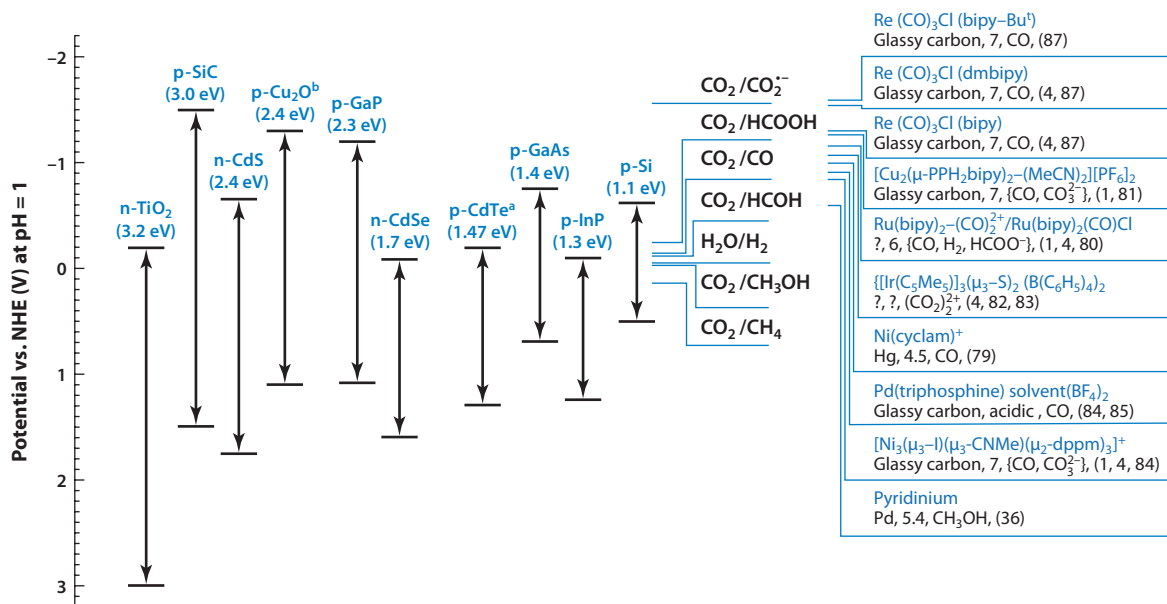


Figure 4

Position of the conduction and valence bands of several semiconductors at pH = 1 versus a normal hydrogen electrode (NHE) (77, 78). Thermodynamic potentials for CO₂ reduction to different products at pH = 1 versus an NHE are shown beside the band edge positions of semiconductors. CO₂ reduction potentials of the homogeneous catalysts are shown at the right. Information presented here (in the form of catalyst, electrode used, pH, product, references) and detailed information about the homogeneous catalysts can be found in References 1, 4, 36, and 79–87. Band edges for p-CdTe are given in Reference 88. Band edges for p-Cu₂O are given in References 89 and 90.

methanol. The greatest difference between water and nonaqueous solvents is the solubility of CO_2 . In nonaqueous solvents, the solubility is 7–8 times higher than in water (10, 93, 94). Methanol, for example, is known to be a physical absorber of CO_2 and is presently used in the Rectisol process in industrial plants (20, 31, 32). Aqueous media further complicate CO_2 reduction, as different CO_2 hydration products are present in water. In water, CO_2 hydration occurs to form carbonic acid, which then undergoes stepwise dissociation to bicarbonate (HCO_3^-) and carbonate (CO_3^{2-}). The predominant species is pH-dependent: CO_2 is dominant at $\text{pH} < 4.5$; HCO_3^- is dominant at $7.5 < \text{pH} < 8.5$; and CO_3^{2-} is dominant at $\text{pH} > 11.5$ (95). This, in turn, affects the thermodynamic potentials for generating certain products, as they are dependent on the form of CO_2 present in solution.

Water, however, is commonly used as a proton source in aprotic solvents for CO_2 reduction. In one study (96), CO_2 solubility was shown not to change with the addition of up to 1% (500 mM) water to acetonitrile but drastically decreased with higher water concentrations. DMF and DMSO performed better than polypropylene carbonate and acetonitrile when mixed with 1% water, as they were better able to suppress competing proton reduction processes (10). Many other differences between aqueous and nonaqueous solutions are factors in efficient CO_2 reduction apart from those mentioned and are discussed further in Section 3.3.

The limitations of CO_2 solubility in water at standard pressures as well as its diffusion limitations set a maximum catalytic current density of 10 mA cm^{-2} for electrochemical reduction of CO_2 (27, 94). CO_2 solubility, and thus maximum catalytic current, can be increased using high-pressure CO_2 environments. High-pressure CO_2 environments offer high catalytic current density and high selectivity over proton reduction for both metal (97, 98) and semiconductor (25, 26) electrodes. Gas-diffusion electrodes (99, 100), as well as other options, have also been explored to increase CO_2 concentration, which is imperative to increase catalytic current densities.

Several metal electrodes have been used for catalytic reduction of CO_2 in both aqueous and nonaqueous media. The catalytic activity of a metal catalyst can be transferred to semiconductor photocathodes through discontinuous films of metals without sacrificing photovoltage. The objective of this approach is to incorporate the stability and catalytic activity of metal particles with semiconducting photocathodes. In a truly photoelectrocatalytic system, when a photoelectrode coupled to a catalyst (metal particles) is run under illumination, the FE versus applied potential has similar behavior to the catalyst alone with a positive shift in the onset voltage called the photovoltage shift. Apart from the photovoltage shift, catalytic activity and product distribution should not be affected by illumination. A detailed description of this type of system is provided in **Supplemental Section 2**.

Surface plasmon effects of nanometallic particles on semiconductor surfaces have not been considered for this type of photocatalytic system, and an introductory note on this topic is included in **Supplemental Section 3**.

3.1. Aqueous Media

Studies by Junfu & Baozhu (15) of CO_2 reduction at (111) p^+/p -Si to formate agree with the selectivity at inert electrodes proposed by Amatore & Savéant (104). In this study by Junfu & Baozhu, the incident illumination intensity was varied up to as high as 73 mW cm^{-2} , though no dark measurements were taken and no flat band potential was reported. The reduction was done in 0.5 M NaSO_4 under a bromine tungsten lamp. At lower pH, proton reduction to hydrogen dominated (FE for $\text{CO}_2 < 5\%$, $\text{pH} \sim 6$), whereas at high pH, CO_2 solubility diminished. Neutral pH yielded ideal conditions for reducing CO_2 with p-Si. The maximum FE was reported to occur at -1.2 V versus a saturated calomel electrode (SCE), but actual values were not given. HCOOH

(FE = 21%) was produced at -1.6 V versus SCE. Electroplated Pb particles prevented proton reduction and shifted the onset of CO_2 reduction positively by 100 mV.

Both p- and n-type GaAs have been used for direct photoelectrochemical reduction of CO_2 and are well known for their ability to produce methanol (101). The mechanism for methanol production has been contentious for years. Sears & Morrison demonstrated that regardless of illumination or applied bias, $(-1 \ -1 \ -1)$ arsenic-rich surfaces of GaAs spontaneously produce CH_3OH , even under conditions of no net current (101). They attributed this to the corrosion of the electrode, which had no effect on the faradaic product, HCOOH (FE $\sim 100\%$) at -0.8 V versus Ag/AgCl.


Reduction of CO_2 on illuminated (111) surface p-CdTe and (100) surface p-InP was performed with various electrolytes at -1.2 V versus SCE (11). InP was found to be more selective for proton reduction (FE $\geq 60\%$) than was CdTe (FE $\geq 38\%$). When tetraalkylammonium electrolytes were used, proton reduction to H_2 decreased on both CdTe (FE $\geq 10\%$) and InP (FE $\geq 25\%$). Yoneyama et al. (11) attributed this to tetraalkylammonium inhibiting proton adsorption by making the electrodes more hydrophobic. Running at more negative potentials decreased selectivity for CO and raised selectivity for both HCOOH and H_2 . CO_2 reduction performed at 0°C increased CO_2 solubility, which increased CO and HCOOH production. When carbonate electrolytes were used, HCOOH selectivity increased, whereas CO selectivity greatly decreased. This can be understood by considering the reaction of $\text{CO}_2^{\cdot-}$ to CO: two disproportionate $\text{CO}_2^{\cdot-}$ radical anions forming CO and CO_3^{2-} . In the presence of an excess of CO_3^{2-} , the back reaction suppresses CO production.

High-pressure reduction of CO_2 on illuminated p-GaAs and (111) plane p-GaP was performed at various potentials and electrolyte conditions (25). On (111) plane p-GaAs at 1 atm of CO_2 and 0.5 M KCl, CO_2 was reduced at -1.29 V versus SCE to HCOOH (FE = 6.7%) and HCHO (FE = 0.59%). At -1.84 V versus SCE, only HCOOH (FE = 15.2%) was produced. On (111) p-GaP at 3 atm CO_2 , with HClO_4 as the supporting electrolyte, total CO_2 reduction gave a low FE (18%) at -1.00 V versus Ag/AgCl but produced a large amount of CH_3OH (FE = 7.2%). With Na_2CO_3 as the supporting electrolyte, reduction of CO_2 at 3.5 atm peaked, with a total FE of 80% at -1.00 V versus Ag/AgCl and with HCOOH as the main product (FE = 74%). Repeating this experiment at 7.5 atm dropped HCOOH selectivity dramatically (FE = 29%), but methanol selectivity increased (FE = 8.2%). The shift toward proton reduction may be attributed to the increased concentration of carbonic acid.

TiO_2 has also been used as a photoelectrode at high pressures with marginal results (26). The highest FE achieved for CO_2 reduction occurred at 8 atm CO_2 at -1.84 V versus Ag/AgCl with HCOOH as the main product (FE = 22%).

Hinogami and coworkers (27, 91, 92) reported photoelectrochemical reduction of CO_2 on Cu, Ag, and Au nanoparticles attached to (100) p-Si. On particulate-Cu/p-Si electrodes, the expected voltage-dependent FEs and discrete photovoltage shifts were obtained under illumination. Cu is a unique catalyst, as it can readily reduce CO_2 beyond HCOOH and CO at higher applied potentials (102). **Figure 5** shows the FE of different products on illuminated particulate-Cu/p-Si photocathodes and dark Cu cathodes versus applied potential. It is evident from the figure that photogenerated electrons are available to particulate-Cu/p-Si for CO_2 reduction with a photovoltage shift of 500 mV versus bare Cu. Similar behavior was observed with particulate-Ag/p-Si and particulate-Au/p-Si photocathodes (tabulated in **Supplemental Table 1**) (27).

Electrodes utilizing Cu and Ru particles on p-GaP have been used to reduce CO_2 under illumination (28). Flaisher et al. (28) employed chopped illumination with both sub-band gap excitations and higher than band gap excitations. At an applied potential of -1.54 V versus SCE, trace amounts of HCOOH were seen, but mostly H_2 was produced. Current enhancement was seen for CO_2 reduction with both Cu and Ru.

 Supplemental Material

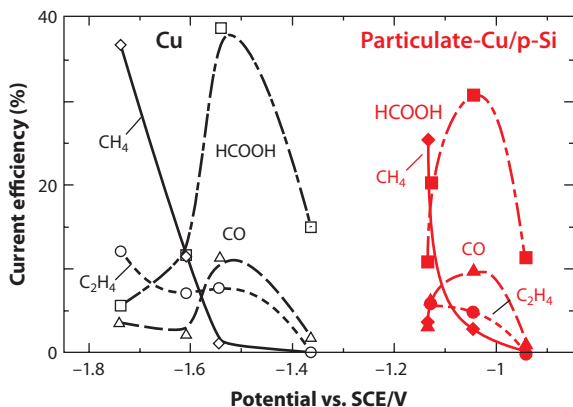


Figure 5

Current efficiencies versus potential for various CO₂ reduction products after potentiostatic electrolyses on particulate-Cu/p-Si and Cu-metal electrodes. Note the similarity in reduction behavior offset by approximately 500 mV. Reprinted with permission from Reference 27. Copyright 1998 American Chemical Society. Abbreviation: SCE/V, saturated calomel electrode per volt.

Some semiconductor materials are not suited for direct contact with aqueous solution due to spontaneous corrosion, but there is still much room for further investigation with semiconductor electrodes, both bare and in conjunction with catalysts.

3.2. Nonaqueous Media

The reduction potentials, current densities, product distributions, and FEs of CO₂ photoelectrochemical reduction on p-Si (10, 17, 33), p-InP (10, 17, 20, 30), p-GaAs (10, 17, 20), and p-GaP (10) in various nonaqueous solvents are tabulated in **Supplemental Table 1**. The main product for CO₂ reduction in most nonaqueous solvents on these semiconductor surfaces was CO with varying FE, except in methanol with a p-GaAs photocathode. In the latter configuration, HCOOH and CH₃COOH were produced with FE similar to that of CO (17). These products are consistent with the CO₂ reduction mechanism proposed for metal electrodes in nonaqueous media in the literature (103). In these cases, comparison between the onset potential of CO₂ reduction and catalytic current density on various semiconductor surfaces is not feasible due to lack of information about illumination intensity.

Much work has been done on p-CdTe photocathodes for CO₂ photoelectrochemical reduction in nonaqueous media by Bockris and coworkers (7, 10, 12, 13, 23, 24). Photoelectrochemical reduction of CO₂ to CO was achieved on (100) p-CdTe at a potential 600–700 mV less negative than a In cathode with 80–85% FE and unit quantum efficiency using 600-nm monochromatic illumination in DMF–5% water with 0.1 M of tetrabutylammonium phosphate (12, 24). When compared with other p-type semiconductors like p-Si, p-GaP, p-InP, and p-GaAs, CdTe was notable for its low CO₂–reduction-onset potential and high quantum efficiency (10). Catalytic current increased with both light intensity (600 nm wavelength, 32 mW cm^{–2}) and CO₂ partial pressure up to 0.5 atm on p-CdTe (10). Saturation of catalytic current and maximum photovoltage occurred at approximately 0.5 atm, which may have been limited by the incident light intensity (32 mW cm^{–2}). A FE of 80–85% was observed for DMF, DMSO, and PC with 5% water as the solvent, whereas acetonitrile had a FE approximately 60% due to its protophobic nature that favors proton reduction (10).

Higher-pressure CO₂ (40 atm) was employed for nonaqueous systems to further improve the catalytic current density. Most efforts using this approach utilized methanol as the solvent (17–19). Only three types of semiconductors (p-Si, p-GaAs, p-InP), each using the (100) surface, were investigated, with the primary focus on (100) p-InP. For (100) p-InP, a catalytic current density of 100–200 mA cm⁻² was achieved. Photoelectrochemical reduction of CO₂ was limited by light intensity and not mass transport of CO₂ (17). Apart from enhanced catalytic current density, the high CO₂ pressure also provided better selectivity for CO₂ over proton reduction for all three semiconducting photocathodes, with the main product being CO. For p-InP, the photostability improved significantly under high CO₂ pressure.

Similar to aqueous media, p-type semiconductors decorated with metal nanoparticles were also examined in nonaqueous solvents for CO₂ photoelectrochemical reduction. Various metal nanoparticles were explored on p-type semiconductors such as p-Si (33), p-InP (30–32), p-GaP (29), and p-CdTe (13). For particulate-Cu/p-Si in 3 M H₂O in acetonitrile, products such as CH₄ and C₂H₄ were observed with a photovoltage shift of 500 mV with respect to Cu (33). These products are characteristic of CO₂ reduction on Cu electrodes. The major product of CO₂ reduction in methanol on a p-InP photocathode modified with metal particles of Au, Ag, Pd, Cu, and Ni was CO, whereas for particulate-Pb/p-InP, the major product was HCOOH (31). A product yield comparison between particulate-Cu/p-InP and particulate-Pb/p-InP suggested that Cu was not acting catalytically on the semiconducting electrode, whereas Pb was. Much improvement is needed in this type of system for CO₂ photoelectrochemical reduction. Most critically, integration of a metal particle's catalytic activity on a p-type semiconductor electrode must be improved to minimize loss of photovoltage.

3.3. The Mechanism of CO₂ Reduction on Semiconductor Surfaces

The three primary products of the reduction of CO₂ are oxalate [(CO₂)₂²⁻], CO, and HCOO⁻/HCOOH. In aqueous solutions and on electrodes not selective for oxalate or CO, HCOO⁻ is the main product. In nonaqueous solutions with relatively low proton concentrations, CO and oxalate are the primary products.

Amatore & Savéant (104) offered some of the earliest mechanistic discussions on selectivity in aqueous media. They stated that on inert electrodes HCOO⁻/HCOOH is the main product. On some electrodes like Cu, CO₂ can be reduced as far as ethanol and methane and the selectivity for these products can be directed by adjusting the working electrode potential (27, 103).

The most energetically demanding and often rate-limiting step is the initial reduction of CO₂ to CO₂⁻. Adsorption onto an electrode surface can allow for both heterogeneous electron transfer and stabilization of the CO₂⁻ species. On transition metals, stabilization occurs through back-bonding from d-orbitals to the antibonding π* orbital of CO₂ (103). This back-donation tends to favor side-on or C-coordinated adsorption.

There is disagreement about whether the many steps involved in CO₂ reduction occur through adsorbed species or in solution away from the surface. Although much work has already been done to discover the intermediates and products involved, the large number of proposed mechanisms shows that more definitive studies are required. For example, Hori et al. (103) and Jitaru et al. (106) disagree on the mechanism for formate production on sp group metals. Although both agree that water is deprotonated by CO₂⁻ to form the carboxyl radical formyloxyl (HCO₂·), they disagree about whether or not this radical remains adsorbed onto the electrode surface. CO₃²⁻ and OH⁻ concentrations with respect to HCOO⁻ production are not discussed in these studies.

Amatore & Savéant (104) also discuss the competing pathways for the primary CO₂ reduction products in media of low proton availability. Their kinetic studies on Pb and Hg electrodes show

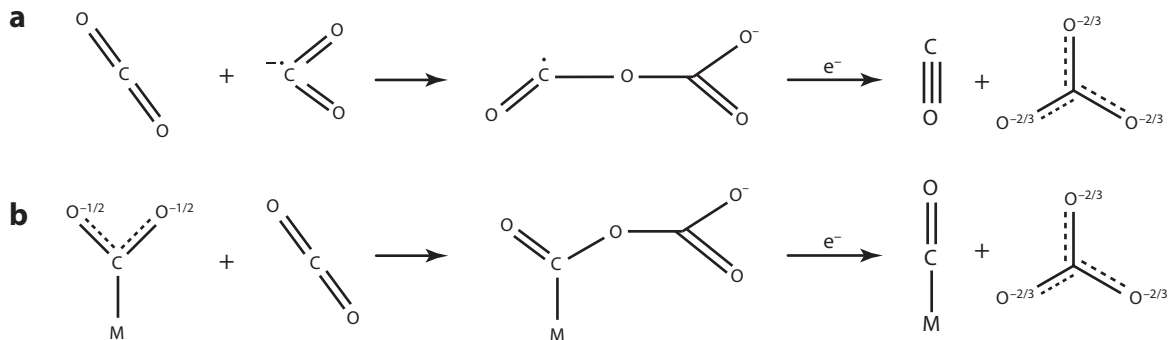


Figure 6

(a) The Savéant-proposed mechanism and (b) the Hori-proposed mechanism for CO production in low proton concentrations or high CO_2 concentrations (103).

that oxalate production occurs through spontaneous formation of a carbon-carbon bond between $\text{CO}_2^{\bullet-}$ anions in solution. For CO, they propose a dimer wherein $\text{CO}_2^{\bullet-}$ bonds with unreduced CO_2 to form an oxygen-carbon bond as depicted in **Figure 6a**. Upon a second reduction, disproportionation of the dimer to CO and CO_3^{2-} occurs. For HCOO^- , the authors propose that $\text{CO}_2^{\bullet-}$ and water react to form HCO_2^{\bullet} and OH^- . Upon a second reduction of the HCO_2^{\bullet} radical, HCOO^- is produced.

Hori et al. (103) propose that C-coordinated CO_2 on metal electrodes may have similar properties to CO_2 in the $\text{Ni}(\text{cyclam})\text{Cl}_2$ catalyst system. They state that electron density is pushed onto the O atoms as opposed to the C atom. As such, the O atoms can form bonds with hydrogen atoms or C atoms from CO_2 .

Tryk et al. (105) used calculations and Tafel plots for CO_2 reduction on InP and particulate metal/carbon electrodes to support the hypothesized intermediate shown in **Figure 6a**. Their thermodynamic calculations for the gaseous species of $\text{CO}_2^{\bullet-}$ and the radical dimer yield a stabilizing energy equivalent to a positive voltage shift of 1.5 V upon dimerization. The authors also demonstrate that tetrabutylammonium ions can increase selectivity for CO_2 reduction on electrode surfaces by making the surface more hydrophobic. Additionally, they propose that surfaces capable of adsorbing CO_2 into a matrix of T-coordinated molecules assist in photoelectrochemical reduction of CO_2 to CO.

Jitaru et al. (106) and Hara et al. (99) both correlate catalytic selectivity to elemental groups of metals. Extensive work on semiconductor electrode materials has not been done, but these studies on metals may shed light on how reduction occurs on plain semiconductor electrodes. The orbital character of the studied electrodes is a good predictor of selectivity. In aqueous solutions, sp metals and d^{10} metals are selective for HCOO^- , whereas d metals are more selective toward CO (97, 106). In nonaqueous media, some sp metals are selective for oxalate, whereas some sp and most d metals are selective for CO (106).

Cu in particular is a unique metal as it can efficiently reduce CO_2 past CO, as adsorbed CO does not easily poison its surface. To understand this mechanism, Peterson et al. (107) used density functional theory to evaluate the free energy landscape for reduction and protonation of adsorbed CO. Their model, which accounts for adsorption sites of protons and the adsorbed products, is in agreement with faradaic selectivity demonstrated in other literature. For a thorough discussion of CO_2 reduction on Cu, refer to Gattrell et al. (102).

4. PHOTOELECTROCHEMICAL REDUCTION OF CO₂ BY SEMICONDUCTOR/MOLECULAR CATALYST JUNCTIONS

The thermodynamic potentials for the proton-assisted multielectron reduction of CO₂ lie within the band gap of the semiconductors (**Figure 4**). However, managing these multielectron multi-proton processes requires a molecular electrocatalyst. Most molecular electrocatalysts for CO₂ reduction operate at a fixed pH, typically under acidic conditions. For several semiconductors, the flat band potential is also a function of pH. The variation is typically 0.059 V/pH units in accordance with the Nernst equation and reflects a change in the voltage across the Helmholtz layer, which is particularly true for semiconductors like InP, GaAs, GaP, and TiO₂ (77, 108). Despite this projected variation, the reduction potential of most molecular electrocatalysts might still be above the conduction band of p-type semiconductors as shown in **Figure 4**.

For ideal semiconductor/liquid junctions, no photoreduction of the redox species above the conduction and below the valence band edge should exist. It has been shown before, however, that the photoreduction of species with redox potentials more negative than the conduction band edges of p-type semiconductors (Ge, Si, InP, GaAs) is feasible (109–112). This phenomenon is explained by Fermi-level pinning and/or unpinning of the band edges, which causes the photovoltage observed for a p-type semiconductor/liquid junction to become independent of the redox potentials of the electroactive species. This pinning leads to photoreduction of molecular electrocatalysts, even if the reduction is above the conduction band edge of the p-type semiconductor, which was shown for the p-Si/Re(bipy-Bu⁺)(CO)₃Cl molecular catalyst junction (37). It can be concluded that as long as the reduction potential of the molecular catalyst is above the valence band edge of the p-type semiconductor, the photoreduction of the molecular electrocatalyst is feasible. Fermi-level pinning also places a limitation on the maximum photovoltage/open circuit voltage for a particular semiconductor/liquid junction to one-half the band gap of the semiconductor (109–112). The stability of the semiconductor photocathode can be further enhanced by surface modification, either by covalent attachment or coating the surface with polymer films of the molecular electrocatalyst. Critical properties and characteristics of photoelectrochemical reduction of CO₂ using semiconductor/molecular electrocatalyst junctions reported in the literature are tabulated in **Supplemental Table 2**.

4.1. Homogenous CO₂ Photoreduction Through p-Type Semiconductor/Molecular Junctions

Bradley & Tysak (113) first showed stable photoreduction of tetraazamacrocyclic metal complexes on a p-Si photocathode. For p-Si/molecular electrocatalyst junctions, photovoltages of 350–400 mV were observed with light to electrical energy conversion efficiency of 0.5 to 1% under noncatalytic conditions. These reduced tetraazamacrocyclic metal complexes were later shown to catalyze the photoreduction of CO₂ to CO on illuminated p-Si (43). The highest efficiency achieved in this system (2 CO:1 H₂, FE = 95 ± 5%) was obtained with 18 mM of [(Me₆[14]aneN₄)Ni^{II}]²⁺ as a molecular catalyst in 1:1 acetonitrile–water solution with 0.1 M LiClO₄ as the supporting electrolyte. However, in completely dry acetonitrile with 0.1 M tetrabutyl ammonium perchlorate, only an equimolar amount of CO and CO₃²⁻ was observed at –1.3 V versus SCE. No information regarding illumination intensity or catalytic current density was provided, making it difficult to calculate efficiency.

Zafrir et al. (42) studied the vanadium V(II)/V(III) redox couple in a highly acidic aqueous medium (114, 115) for photoreduction of CO₂ on a p-GaAs photocathode. V(II) does not electrocatalytically reduce CO₂, which resulted in poor FEs of less than 2% (42). Parkinson & Weaver

Supplemental Material

(41) overcame this by introducing a formate dehydrogenase enzyme as a catalyst for CO₂ reduction to formate. In this work, the enzyme was used in conjunction with methyl viologen (MV) as an electron relay on a p-InP photoelectrode (41). The advantages of a p-InP/(MV²⁺/MV¹⁺)/biological catalyst system are low overpotential for CO₂ reduction, selectivity, and excellent FE. The disadvantages of this system include instability of the formate hydrogenase enzyme and low efficiency.

Tinnemans et al. (65) reported CO₂ photoreduction by p-GaP/ and p-GaAs/tetraaza-macrocyclic Co(II) and Ni(II) junctions. However, no stable photoreduction of the catalysts was observed on p-GaP and no photovoltage was observed for the p-GaAs/catalyst junction. Beley et al. (40) and Petit et al. (39) also reported the photoreduction of CO₂ on p-GaAs and p-GaP photocathodes with Ni(cyclam)²⁺ (cyclam = 1,4,8,11-tetraazacyclotetradecane) as the molecular catalyst. A comprehensive review and further investigation was reported later by Petit et al. (38) on p-GaAs (111) and p-GaP (111)/Ni(cyclam)²⁺ molecular catalyst junctions in aqueous media. CO₂ photoreduction with Ni(cyclam)²⁺ on p-GaP was achieved as low as 200 mV below the thermodynamic potential for CO₂ to CO reduction, at -0.2 V versus an NHE. Selectivity of CO over H₂ was found to be between 1 and 2 for p-GaAs and between 5 and 10 for p-GaP with a FE of 80–100% (38–40). The difference in selectivity for p-GaAs and p-GaP could be due to their inherent surface chemistry characteristics. The best performance was observed for 5 mM of catalyst at 20 mW cm⁻² light intensity, which was explained by the occupation of accessible sites on the semiconductor surface by Ni(cyclam)²⁺ or other intermediate species. No efficiency data were provided for this case. More work is necessary to fully understand the potential of the p-type semiconductor/Ni(cyclam)²⁺ system.

Barton et al. (36) reported another system consisting of a p-GaP (111) photocathode and a soluble pyridinium molecular catalyst for direct selective photoreduction of CO₂ to methanol at 300 mV of underpotential at pH 5.2 with 63–100% FE. In this system, an overall conversion efficiency of 11% was achieved using an illumination wavelength of 365 nm at 6.5 mW cm⁻². FE of methanol formation decreased and catalytic current density increased as the applied underpotential decreased, which was explained by competing proton/water reduction processes. Apart from p-GaP, pyridinium was only active with platinum group metal electrodes and inherently has low catalytic current density and FE for methanol formation.

Selective photoreduction of CO₂ to CO using a hydrogen terminated p-Si/Re(bipy-Bu^t)(CO)₃Cl (bipy-Bu^t = 4,4'-di-tert-butyl-2,2'-bipyridine) molecular catalyst junction was recently reported with a photovoltage exceeding 600 mV (37). The system had a FE of 97 ± 3% for selective photoreduction of CO₂ to CO. Around 10% of the light energy was used for the photoreduction using either polychromatic or monochromatic light (661 nm) with a maximum catalytic current density of 31 mA cm⁻². The most important aspect of this system was that the catalytic current density was only limited by the monochromatic light intensity (661 nm) up to 95 mW cm⁻² (Figure 7).

4.2. Theoretical Treatment of Homogenous CO₂ Photoreduction Through p-Type Semiconductor/Molecular Junctions

Figure 8 shows a schematic of photoelectrochemical CO₂ reduction by a p-type semiconductor/molecular junction using p-Si and Re(bipy-Bu^t)(CO)₃Cl as an example. There are three critical steps involved in this process: (a) charge carrier generation and separation in the semiconductor, (b) heterogeneous charge transfer to the molecular electrocatalyst, and (c) homogeneous catalysis. The total photocurrent density at an illuminated p-semiconductor/liquid junction (assuming no recombination of photogenerated carriers within the diffusion layer and fast charge transfer

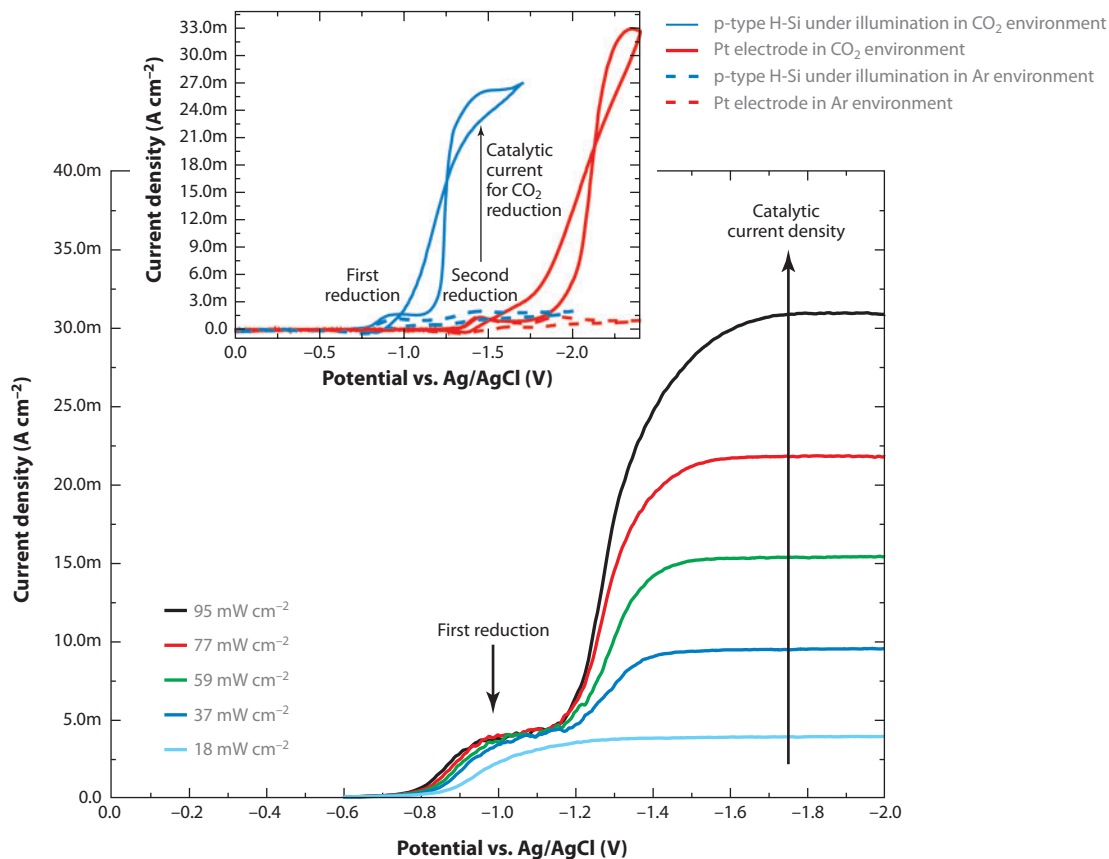


Figure 7

Current density-voltage characteristic of a hydrogen-terminated p-Si/Re(bipy-Bu³)(CO)₃Cl molecular catalyst junction under CO₂ with varying monochromatic light (661 nm) intensity. (Inset) Cyclic voltammograms of Re(bipy-Bu³)(CO)₃Cl under CO₂ and Ar atmospheres on hydrogen-terminated p-Si photocathodes (blue) and Pt electrodes (red).

between the semiconductor and redox species) is given by Equation 7 (116):

$$J_{total} = eQ \left[1 - \frac{e^{(-\alpha W_S)}}{1 + \alpha Z_p} \right] + en_0 \left(\frac{D_n}{Z_p} \right). \quad (7)$$

In this equation, Q is the photon flux, α the absorption coefficient, W_S the depletion width, D_n the diffusion coefficient of the electron in the semiconductor, n_0 the equilibrium concentration of electrons, and Z_p the electron diffusion length in the semiconductor.

Limiting catalytic current density for homogeneous catalysis with EC'-type mechanism is given by Equation 8 (85, 117, 118):

$$J_{\infty} = nFC_0^*(Dk'C_Z^*)^{1/2}. \quad (8)$$

In this equation, n is the number of electrons involved in the reduction (2 for CO₂ reduction to CO), F the faradaic constant, C_0^* the catalyst concentration, D the diffusion coefficient of catalyst, k' the catalytic rate constant, and C_Z^* the substrate concentration (CO₂ concentration). Equation 8 is derived for a quiescent solution with the assumption that the substrate concentration

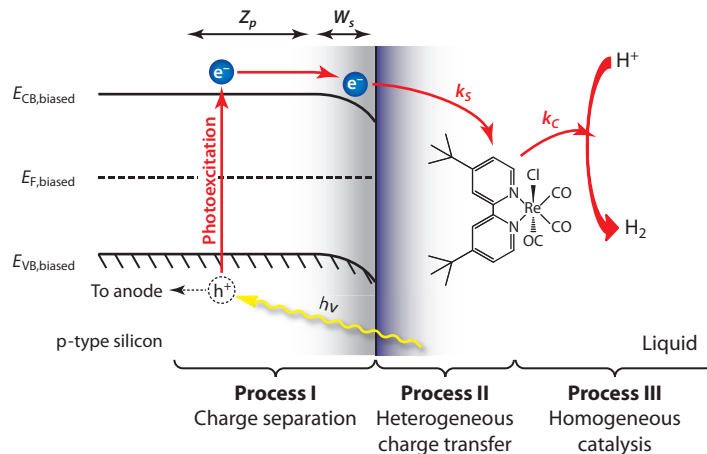


Figure 8

A schematic of CO_2 photoreduction by a p-type semiconductor/molecular junction with p-Si and a $\text{Re}(\text{bipy-Bu})_3(\text{CO})_3\text{Cl}$ molecular electrocatalyst junction as an example. The figure shows three processes involved in photoreduction of CO_2 by a p-type semiconductor/molecular catalyst junction.

is higher than the catalyst concentration and that there is fast charge transfer between the electrode and molecular catalyst.

From Equations 7 and 8, it is clear that for a given p-type semiconductor/molecular electrocatalyst junction, the photocurrent density depends on incoming light intensity, whereas the limiting catalytic current density depends on catalyst concentration. To maximize photocatalytic current density, the photocurrent density and limiting catalytic current must be closely matched. Therefore, for a given semiconductor/molecular electrocatalyst junction, the catalyst concentration must be chosen corresponding to the illumination intensity used and the catalyst's TOF.

Based on the expressions for efficiency (see **Supplemental Section 1**), it is evident that the overpotential of CO_2 photoelectrochemical reduction is usually unfavorable. A molecular catalyst with low or no overpotential for CO_2 reduction and high TOF would be essential for direct conversion of light energy to chemical energy. However, most of the molecular catalysts with high TOFs also have high overpotentials (1, 4) (**Figure 4**). The integrated maximum photocurrent under Air Mass 1.5 illumination using the conventional Shockley–Queisser limit for solar energy conversion for p-Si (1.12 eV), p-InP (1.3 eV), p-GaAs (1.4 eV), and p-GaP (2.3 eV) are 44.0 mA cm^{-2} , 37.0 mA cm^{-2} , 32.5 mA cm^{-2} and 9.0 mA cm^{-2} , respectively (78). Therefore, for low band gap semiconductors, obtaining high photocurrent densities requires the use of a molecular catalyst with high TOFs. Given Equation 8, it is also possible to increase the limiting catalytic current density for a given molecular catalyst by increasing its concentration. In this case, however, two issues arise: higher catalyst concentration will lead to an increase in light absorption by the solution, and the solubility of the catalyst is limited in any given solvent. Possible improvement in conversion efficiency can be achieved by using multijunction electrodes, which is proposed and discussed later in this review.

Supplemental Material

4.3. Heterogeneous CO_2 Photoreduction by Molecular Catalysts Anchored to the Semiconductor Surface

On account of competing advantages of homogeneous catalysts (selectivity, tunability) and heterogeneous catalysts (robustness, easy separation of products from catalysts), there is considerable

interest in “heterogenizing” homogeneous catalysts, by covalently linking them to surfaces. There have been several reports regarding surface modification of dark electrodes using the polymeric form of the molecular catalysts and/or enzymes for electrochemical reduction of CO_2 to various products (4, 44, 119–134). These modified dark electrodes have several advantages: control over the active site environment for better performance (119, 135); prevention of aggregation or dimerization of the molecular catalyst, which leads to higher TONs (136); efficient charge transfer to the molecular catalyst; usability of water-insoluble molecular catalysts in aqueous media once anchored to electrodes (137); and stabilization of the catalyst and electrode (138–141). The physical nature of these junctions is similar to a semiconductor/liquid junction with unbound molecular electrocatalysts (142). Molecular catalyst surface-modified semiconductors can be subdivided into two categories: polymeric backbone attachment, and direct anchoring to the semiconductor surface.

Aurian-Blajeni et al. (46) reported CO_2 photoreduction on polyaniline-coated p-Si at -1.0 V versus SCE in aqueous solution. In this report, formic acid and formaldehyde were formed with a FE of 20–30% after bulk electrolysis performed at -1.9 V versus SCE, with power conversion efficiency (see **Supplemental Section 1**) of 3–4%. Cabrera & Abruña (44) reported CO_2 photoreduction to CO by an electropolymerized molecular catalyst ($\text{Re}(\text{CO})_3(4\text{-vinyl}, 4'\text{-methyl-2,2'-bipyridine})\text{Cl}$) on p-Si and p- WSe_2 . A lower TON of 450 was reported compared with electropolymerized molecular catalyst on a metal surface (600 for surface-modified Pt) with FE of 100%. No calculations for conversion efficiency were made, as no information was provided about the illumination intensity for these systems.

Arai et al. (45) reported CO_2 photoreduction to formate in an aqueous medium by a p-InP/ruthenium-complex polymer junction. The ruthenium-complex polymer (RCP) used was $[\text{Ru}(\text{L-L})(\text{CO})_2]_n$ (L-L = diimine ligand), which was previously reported as an electropolymerized catalyst (L-6) on Pt and vitreous carbon electrodes (127). CO_2 photoreduction was achieved at a potential -800 mV less negative versus glassy carbon/RCP (45). The best FE (63%) for formate production was obtained for a p-InP/RCP junction prepared by a two-step polymerization of RCP (127), which stabilized the polymeric film when under a cathodic bias (127) and in aqueous media (45). Low FE was reported in the above case due to competing H_2 - and CO-generation processes. No supporting electrolyte was added, which can result in high cell resistance and resistive losses.

Unlike dark electrodes, there are not many reports of semiconductor photocathodes modified with polymeric films. This could be due to the absorption of incoming light as well as a high number of photogenerated-carrier-trapping sites in the polymeric films.

To the best of our knowledge, there are no reports of photoelectrochemical CO_2 reduction by molecular catalysts directly attached to semiconductor surfaces. Recently, however, CO_2 reduction by molecular electrocatalysts/enzymes attached to semiconductor surface has been reported (143–146). Two of these report photocatalytic reduction of CO_2 to formate (144) or CO (145). Both systems are analogous to homogeneous photocatalytic reduction of CO_2 by photosensitizers and molecular catalysts discussed in Section 2. In the above cases, the molecular catalyst is either adsorbed or electrostatically attached to the semiconductor surface. A recent theoretical study (146) has shown covalent bond formation between $\text{Re}(\text{CO})_3\text{Cl}(\text{dcbpy})$ ($\text{dcbpy} = 4,4'\text{-dicarboxy-2,2'-bipyridine}$) and the TiO_2 rutile (001) surface but failed to recognize that $\text{Re}(\text{CO})_3\text{Cl}(\text{dcbpy})$ has no catalytic activity for CO_2 reduction (87).

Substantially more effort in molecular catalysts covalently bound to semiconductor surfaces is needed, with special consideration given to the accessibility of the catalytic site and its structural/activity requirements. The large cathodic bias required for photoelectrochemical reduction of CO_2 can cause adsorbed or electrostatically attached molecular catalysts to become loosened

from the semiconductor surface. Therefore, well-designed covalent attachment of the catalyst is imperative for stability of this method.

5. PROSPECT

Multijunction photoelectrolysis cells are presently used to overcome the high potential that is associated with water splitting. Four types of these cells are currently used: p/n junction photoelectrolysis cells, photoanode-PV cells, photocathode-PV cells, and PV photoelectrolysis cells (147–150). An excellent analysis of these cells is presented by Walter et al. (78) in their review on solar water splitting. Similar efforts for CO₂ photoreduction are lacking.

Of note, the PV photoelectrolysis cell has a photovoltage that is independent of pH, which is important for pH-sensitive catalyst-mediated CO₂ reduction. This cell can also be easily modified with CO₂ reduction catalysts selective for specific products. In addition, this type of cell utilizes a majority of the solar spectra and has a high photovoltage, unlike wide band gap semiconductor photoelectrodes. The total thermodynamic potential to reduce CO₂ to products like CH₃OH or CH₄ and to oxidize water to oxygen is only approximately 1.2 V. In practice, however, the applied potential required for simultaneous reduction of CO₂ and oxidation of water is at least 2.0 V. Water oxidation using PV electrodes has been explored by Yamane et al. (150). Photovoltages of 2.2 V and 1.7 V were reported with n-Si/p-CuI/ITO/n-i-p a-Si/n-p GaP/ITO/RuO₂ and n-i-p a-Si/n-p GaP/ITO/RuO₂, respectively, with 0.1 M Na₂SO₄ (pH = 6.3) as the supporting electrolyte.

It is possible for this technology to be used as a wireless, monolithic, two-compartment PV-type photoelectrolysis cell with single dual face photoelectrode. A proposed cell using a CO₂ reduction catalyst/FTO/n-Si/p-CuI/ITO/n-i-p a-Si/n-p GaP/ITO/water-oxidation catalyst electrode configuration is shown in **Figure 9**. The fabrication cost of the electrode may be high; however, the simple structure of the cell, the ease of product separation, and the robustness of the electrode could lead to a long operation time and an environmentally friendly process. There are two major challenges for these types of cells: identifying catalysts based on earth-abundant materials that have low overpotentials for CO₂ reduction and water oxidation, and finding a reliable and robust proton-exchange membrane. It is clear that the advantages of this type of system outweigh the cost. Therefore, it is imperative to explore and adopt water-splitting/hydrogen-generation technology for solar splitting of CO₂ for liquid fuel applications as well as to broaden the search for new robust, selective, and efficient catalytic systems. In the quest for new catalysts, combinatorial approaches will prove useful for both discovery and optimization of new catalysts (151).

6. EXPERIMENTAL AND THEORETICAL CHALLENGES

Virtually every approach under consideration for the photochemical or photoelectrochemical reduction of CO₂ to fuels requires catalysts to facilitate the formation and cleavage of chemical bonds. In general, the required catalysts fall into three classifications: (a) They already exist and work but are too rare/costly to be scaled up; (b) they already exist but in forms that are not optimal or practical for adaptation to an integrated solar fuels system; (c) they do not exist and await discovery. The challenges in catalysis are large indeed. The best photovoltaic or photoelectrochemical materials can sustain current densities of 10–20 mA cm⁻². In contrast, for a two-electron process, a monolayer of catalyst with a TOF of 1,000 s⁻¹ will sustain a current density of only 0.1 mA cm⁻². Presently, no electrocatalysts for the reduction of CO₂ function at low overpotential with high selectivity, and hence would be useful for a large-scale system. The work reviewed here on the photochemical and photoelectrochemical reduction of CO₂ illustrates many of the difficult issues

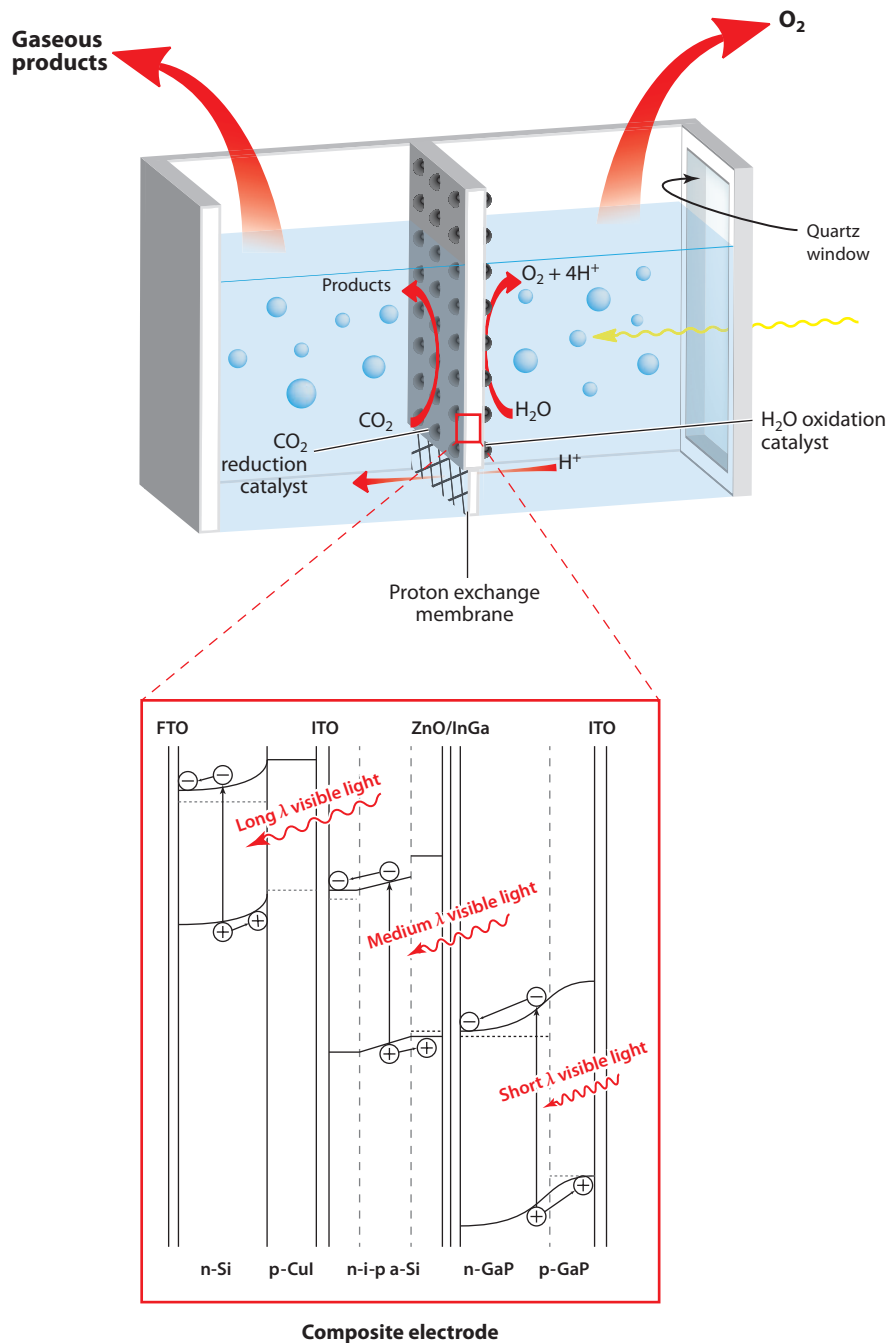


Figure 9

Schematic of a proposed photochemical cell with a multijunction tandem photoelectrode for CO₂ photoreduction. The electrode structure is adapted from Yamane et al. (150). Abbreviations: FTO, fluorine-doped tin oxide; ITO, indium tin oxide.

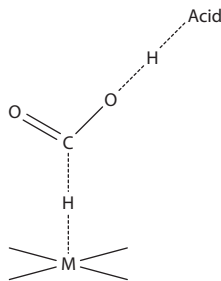


Figure 10

Example of CO₂ activation by M-H and an acidic proton to produce formic acid.

in CO₂ reduction chemistry. How does one obtain a metal center that is sufficiently nucleophilic to bind CO₂ at low potentials (avoiding negative oxidation states like Re(-1), for example)? Can this be done with earth-abundant metals? The most costly thermodynamic issue appears to be CO₂ binding to the metal center. The most costly kinetic issue appears to be C-O bond breaking in the metal-CO₂ complex. There is evidence that Lewis acid cocatalysts can be used to accelerate CO₂ reduction catalysis, but the thermodynamic issue of a highly negative reduction potential remains.

Future experimental and theoretical work needs to examine whether catalysts that find low-energy transition states for CO₂ reduction are viable. Groups that stabilize negative charge on the CO₂ O-atoms should lessen the metal nucleophilicity requirement of the metal center and could also lower the barrier for C-O bond breaking. How much these factors can increase the efficiency of the CO₂ reduction catalysts needs to be determined, followed by the question of whether the oxidation state and reduction potential need to be as negative as they are for many of the systems reported. This may be done by computing CO₂ affinities for a variety of mid- to late-transition metal complexes for which the reduction potential and metal nucleophilicity can be varied by ligand substitution. The theory will need to be tested by experiment, and new complexes will need to be prepared to refine predictive abilities. From both thermodynamic and kinetic points of view, PCET mechanisms for CO₂ reduction appear to be more efficient. In some PCETs to CO₂, it is a nucleophilic metal hydride and not the nucleophilic metal itself that engages CO₂ (**Figure 10**). Of course, this transition state produces formic acid, and if more reduced species such as methanol are desired, then the H donor/acceptor properties required to reduce formic acid also need to be identified.

Hydricities have now been measured for many transition metal (152) and NADH-like (153) hydride donors, and they have been applied to explain the thermodynamics of proton reduction catalysis. Hydricities have only recently been applied to CO₂ reduction (154). The expanding database of hydricities should be combined with theoretical studies of transition states for different types of CO₂ reduction to bring a more rational set of design principles to the problem of CO₂ reduction catalysis.

Theoretical approaches to understanding the energy landscapes of intermediates formed in the electrochemical reduction of CO₂ on copper surfaces have become available recently (107). This work is providing a clearer understanding of the potential dependence of the thermodynamic stability of key intermediates in the electrochemical reduction of CO₂, and thereby the potential dependence of branching ratios for CO₂ reduction to different products. It appears that computational approaches to the kinetic barriers to key intermediates in the electrochemical reduction of CO₂ at other metal and semiconducting surfaces will also become available. One particularly

promising approach to photochemical and photoelectrochemical reduction of CO₂ in the future will be to address the kinetic and thermodynamic stability of the rate-limiting CO₂ reduction intermediates on electrode surfaces with molecular catalysts selected to accelerate the reduction of those intermediates.

DISCLOSURE STATEMENT

The authors are not aware of any affiliations, memberships, funding, or financial holdings that might be perceived as affecting the objectivity of this review.

LITERATURE CITED

1. Benson EE, Kubiak CP, Sathrum AJ, Smieja JM. 2009. Electrocatalytic and homogeneous approaches to conversion of CO₂ to liquid fuels. *Chem. Soc. Rev.* 38:89–99
2. Kedzierzawski P, Augustynski J. 1994. Poisoning and activation of the gold cathode during electroreduction of CO₂. *J. Electrochem. Soc.* 141:L58–60
3. Leitner W. 1996. The coordination chemistry of carbon dioxide and its relevance for catalysis: a critical survey. *Coord. Chem. Rev.* 153:257–84
4. Savéant J-M. 2008. Molecular catalysis of electrochemical reactions: mechanistic aspects. *Chem. Rev.* 108:2348–78
5. Halmann M. 1978. Photoelectrochemical reduction of aqueous carbon dioxide on p-type gallium phosphide in liquid junction solar cells. *Nature* 275:115–16
6. Taniguchi Y, Yoneyama H, Tamura H. 1982. Photoelectrochemical reduction of carbon dioxide at p-type gallium phosphide electrodes in the presence of crown ether. *Bull. Chem. Soc. Jpn.* 55:2034–39
7. Aurian-Blajeni B, Ahsan Habib M, Taniguchi I, Bockris JOM. 1983. The study of adsorbed species during the photoassisted reduction of carbon dioxide at a p-CdTe electrode. *J. Electroanal. Chem.* 157:399–404
8. Canfield D, Frese JKW. 1983. Reduction of carbon dioxide to methanol on n- and p-GaAs and p-InP: effect of crystal face, electrolyte and current density. *J. Electrochem. Soc.* 130:1772–73
9. Frese KW Jr, Canfield D. 1984. Reduction of CO₂ on n-GaAs electrodes and selective methanol synthesis. *J. Electrochem. Soc.* 131:2518–22
10. Taniguchi I, Aurian-Blajeni B, Bockris JOM. 1984. The reduction of carbon dioxide at illuminated p-type semiconductor electrodes in nonaqueous media. *Electrochim. Acta* 29:923–32
11. Yoneyama H, Sugimura K, Kuwabata S. 1988. Effects of electrolytes on the photoelectrochemical reduction of carbon dioxide at illuminated p-type cadmium telluride and p-type indium phosphide electrodes in aqueous solutions. *J. Electroanal. Chem.* 249:143–53
12. Bockris JOM, Wass JC. 1989. The photoelectrocatalytic reduction of carbon dioxide. *J. Electrochem. Soc.* 136:2521–28
13. Bockris JOM, Wass JC. 1989. On the photoelectrocatalytic reduction of carbon dioxide. *Mater. Chem. Phys.* 22:249–80
14. Noda H, Yamamoto A, Ikeda S, Maeda M, Ito K. 1990. Influence of light intensity on photoelectroreduction of CO₂ at a p-GaP photocathode. *Chem. Lett.* 19:1757–60
15. Junfu L, Baozhu C. 1992. Photoelectrochemical reduction of carbon dioxide on a p+/p-Si photocathode in aqueous electrolyte. *J. Electroanal. Chem.* 324:191–200
16. Ikeda S, Yamamoto A, Noda H, Maeda M, Ito K. 1993. Influence of surface treatment of the p-GaP photocathode on the photoelectrochemical reduction of carbon dioxide. *Bull. Chem. Soc. Jpn.* 66:2473–77
17. Hirota K, Tryk DA, Yamamoto T, Hashimoto K, Okawa M, Fujishima A. 1998. Photoelectrochemical reduction of CO₂ in a high-pressure CO₂ + methanol medium at p-type semiconductor electrodes. *J. Phys. Chem. B* 102:9834–43
18. Hirota K, Tryk DA, Hashimoto K, Okawa M, Fujishima A. 1998. Photoelectrochemical reduction of CO₂ at high current densities at p-InP electrodes. *J. Electrochem. Soc.* 145:L82–84
19. Hirota K, Tryk DA, Hashimoto K, Okawa M, Fujishima A. 1998. Photoelectrochemical reduction of highly concentrated CO₂ in methanol solution. See Ref. 155, pp. 589–92

20. Kaneco S, Katsumata H, Suzuki T, Ohta K. 2006. Photoelectrochemical reduction of carbon dioxide at p-type gallium arsenide and p-type indium phosphide electrodes in methanol. *Chem. Eng. J.* 116:227–31
21. Le M, Ren M, Zhang Z, Sprunger PT, Kurtz RL, Flake JC. 2011. Electrochemical reduction of CO₂ to CH₃OH at copper oxide surfaces. *J. Electrochem. Soc.* 158:E45–49
22. Ono H, Yokosuka A, Tasiro T, Morisaki H, Yugo S. 2002. Characterization of diamond-coated Si electrodes for photoelectrochemical reduction of CO₂. *New Diam. Front. Carbon Technol.* 12:141–44
23. Taniguchi I, Aurian-Blajeni B, Bockris JOM. 1984. The mediation of the photoelectrochemical reduction of carbon dioxide by ammonium ions. *J. Electroanal. Chem.* 161:385–88
24. Taniguchi I, Aurian-Blajeni B, Bockris JOM. 1983. Photo-aided reduction of carbon dioxide to carbon monoxide. *J. Electroanal. Chem. Interfacial Electrochem.* 157:179–82
25. Aurian-Blajeni B, Halmann M, Manassen J. 1983. Electrochemical measurement on the photoelectrochemical reduction of aqueous carbon dioxide on p-gallium phosphide and p-gallium arsenide semiconductor electrodes. *Solar Energy Mater.* 8:425–40
26. Halmann M, Aurian-Blajeni B. 1994. Electrochemical reduction of carbon dioxide at elevated pressure on semiconductor electrodes in aqueous solution. *J. Electroanal. Chem.* 375:379–82
27. Hinogami R, Nakamura Y, Yae S, Nakato Y. 1998. An approach to ideal semiconductor electrodes for efficient photoelectrochemical reduction of carbon dioxide by modification with small metal particles. *J. Phys. Chem. B* 102:974–80
28. Flaisher H, Tenne R, Halmann M. 1996. Photoelectrochemical reduction of carbon dioxide in aqueous solutions on p-GaP electrodes: an a.c. impedance study with phase-sensitive detection. *J. Electroanal. Chem.* 402:97–105
29. Ikeda S, Saito Y, Yoshida M, Noda H, Maeda M, Ito K. 1989. Photoelectrochemical reduction products of carbon dioxide at metal coated p-GaP photocathodes in non-aqueous electrolytes. *J. Electroanal. Chem. Interfacial Electrochem.* 260:335–45
30. Noda HIS, Saito Y, Nakamura T, Maeda M, Ito K. 1989. Photoelectrochemical reduction of carbon dioxide at metal-coated p-InP photocathodes. *Denki Kagaku* 57:1117–20
31. Kaneco S, Katsumata H, Suzuki T, Ohta K. 2006. Photoelectrocatalytic reduction of CO₂ in LiOH/methanol at metal-modified p-InP electrodes. *Appl. Catal. B* 64:139–45
32. Kaneco S, Ueno Y, Katsumata H, Suzuki T, Ohta K. 2009. Photoelectrochemical reduction of CO₂ at p-InP electrode in copper particle-suspended methanol. *Chem. Eng. J.* 148:57–62
33. Nakamura Y, Hinogami R, Yae S, Nakato Y. 1998. Photoelectrochemical reduction of CO₂ at a metal-particle modified p-Si electrode in non-aqueous solutions. See Ref. 155, pp. 565–68
34. Ikeda S, Yoshida M, Ito K. 1985. Photoelectrochemical reduction products of carbon dioxide at metal coated p-GaP photocathodes in aqueous electrolytes. *Bull. Chem. Soc. Jpn.* 58:1353–57
35. Cottineau T, Morin M, Belanger D. 2009. Modification of p-type silicon for the photoelectrochemical reduction of CO₂. *ECS Trans.* 19:1–7
36. Barton EE, Rampulla DM, Bocarsly AB. 2008. Selective solar-driven reduction of CO₂ to methanol using a catalyzed p-GaP based photoelectrochemical cell. *J. Am. Chem. Soc.* 130:6342–44
37. Kumar B, Smieja JM, Kubiak CP. 2010. Photoreduction of CO₂ on p-type silicon using Re(bipy-But)(CO)₃Cl: photovoltages exceeding 600 mV for the selective reduction of CO₂ to CO. *J. Phys. Chem. C* 114:14220–23
38. Petit J-P, Chartier P, Beley M, Deville J-P. 1989. Molecular catalysts in photoelectrochemical cells: study of an efficient system for the selective photoelectroreduction of CO₂: p-GaP or p-GaAs/Ni(cyclam)²⁺, aqueous medium. *J. Electroanal. Chem.* 269:267–81
39. Petit JP, Chartier P, Beley M, Sauvage JP. 1987. Selective photoelectrochemical reduction of CO₂ to CO in an aqueous medium on p-GaP, mediated by Ni cyclam²⁺. *Nouv. J. Chim.* 11:751
40. Beley M, Collin J-P, Sauvage J-P, Petit J-P, Chartier P. 1986. Photoassisted electro-reduction of CO₂ on p-GaAs in the presence of Ni cyclam²⁺. *J. Electroanal. Chem.* 206:333–39
41. Parkinson BA, Weaver PF. 1984. Photoelectrochemical pumping of enzymatic CO₂ reduction. *Nature* 309:148–49
42. Zafrir M, Ulman M, Zuckerman Y, Halmann M. 1983. Photoelectrochemical reduction of carbon dioxide to formic acid, formaldehyde and methanol on p-gallium arsenide in an aqueous V(II)-V(III) chloride redox system. *J. Electroanal. Chem.* 159:373–89

43. Bradley MG, Tysak T, Graves DJ, Viachopoulos NA. 1983. Electrocatalytic reduction of carbon dioxide at illuminated p-type silicon semiconducting electrodes. *J. Chem. Soc. Chem. Commun.* 7:349–50
44. Cabrera CR, Abruña HD. 1986. Electrocatalysis of CO₂ reduction at surface modified metallic and semiconducting electrodes. *J. Electroanal. Chem.* 209:101–7
45. Arai T, Sato S, Uemura K, Morikawa T, Kajino T, Motohiro T. 2010. Photoelectrochemical reduction of CO₂ in water under visible-light irradiation by a p-type InP photocathode modified with an electropolymerized ruthenium complex. *Chem. Commun.* 46:6944–46
46. Aurian-Blajeni B, Taniguchi I, Bockris JOM. 1983. Photoelectrochemical reduction of carbon dioxide using polyaniline-coated silicon. *J. Electroanal. Chem. Interfacial Electrochem.* 149:291–93
47. Bilgen E. 2001. Solar hydrogen from photovoltaic-electrolyzer systems. *Energy Convers. Manag.* 42:1047–57
48. Gibson TL, Kelly NA. 2010. Predicting efficiency of solar powered hydrogen generation using photovoltaic-electrolysis devices. *Int. J. Hydrog. Energy* 35:900–11
49. Atlam O, Barbir F, Bezmalinovic D. 2011. A method for optimal sizing of an electrolyzer directly connected to a PV module. *Int. J. Hydrog. Energy* 36:7012–18
50. Ogura K, Yamada M, Nakayama M, Endo N. 1998. Electrocatalytic reduction of CO₂ to worthier compounds on a functional dual-film electrode with a solar cell as the energy source. See Ref. 155, pp. 207–12
51. Ogura K, Yoshida I. 1987. Electrocatalytic reduction of carbon dioxide to methanol. VI. Use of a solar cell and comparison with that of carbon monoxide. *Electrochim. Acta* 32:1191–95
52. Ogura K, Yoshida I. 1986. Catalytic conversion of CO and CO₂ into methanol with a solar cell. *J. Mol. Catal.* 34:309–11
53. Halmann M, Ulman M, Aurian-Blajeni B. 1983. Photochemical solar collector for the photoassisted reduction of aqueous carbon dioxide. *Solar Energy* 31:429–31
54. Bard AJ, Fox MA. 1995. Artificial photosynthesis: solar splitting of water to hydrogen and oxygen. *Acc. Chem. Res.* 28:141–45
55. Delacourt C, Ridgway PL, Kerr JB, Newman J. 2008. Design of an electrochemical cell making syngas (CO + H₂) from CO₂ and H₂O reduction at room temperature. *J. Electrochem. Soc.* 155:B42–49
56. Durham B, Caspar JV, Nagle JK, Meyer TJ. 1982. Photochemistry of Ru(bpy)₃²⁺. *J. Am. Chem. Soc.* 104:4803–10
57. Doherty MD, Grills DC, Muckerman JT, Polyansky DE, Fujita E. 2010. Toward more efficient photochemical CO₂ reduction: use of scCO₂ or photogenerated hydrides. *Coord. Chem. Rev.* 254:2472–82
58. Morris AJ, Meyer GJ, Fujita E. 2009. Molecular approaches to the photocatalytic reduction of carbon dioxide for solar fuels. *Acc. Chem. Res.* 42:1983–94
59. Takeda H, Ishitani O. 2010. Development of efficient photocatalytic systems for CO₂ reduction using mononuclear and multinuclear metal complexes based on mechanistic studies. *Coord. Chem. Rev.* 254:346–54
60. Grodkowski J, Neta P. 2000. Cobalt corrin catalyzed photoreduction of CO₂. *J. Phys. Chem. A* 104:1848–53
61. Grodkowski J, Neta P, Fujita E, Mahammed A, Simkhovich L, Gross Z. 2002. Reduction of cobalt and iron corroles and catalyzed reduction of CO₂. *J. Phys. Chem. A* 106:4772–78
62. Grodkowski J, Dhanasekaran T, Neta P, Hambright P, Brunschwig BS, et al. 2000. Reduction of cobalt and iron phthalocyanines and the role of the reduced species in catalyzed photoreduction of CO₂. *J. Phys. Chem. A* 104:11332–39
63. Craig CA, Spreer LO, Otvos JW, Calvin M. 1990. Photochemical reduction of carbon dioxide using nickel tetraazamacrocycles. *J. Phys. Chem.* 94:7957–60
64. Kimura E, Bu X, Shionoya M, Wada S, Maruyama S. 1992. A new nickel(II) cyclam (cyclam = 1,4,8,11-tetraazacyclotetradecane) complex covalently attached to tris(1,10-phenanthroline)ruthenium(2+). A new candidate for the catalytic photoreduction of carbon dioxide. *Inorg. Chem.* 31:4542–46
65. Tinnemans AHA, Koster TPM, Thewissen DHMW, Mackor A. 1984. Tetraaza-macrocyclic cobalt(II) and nickel(II) complexes as electron-transfer agents in the photo(electro)chemical and electrochemical reduction of carbon dioxide. *Recl. Trav. Chim. Pays-Bas* 103:288–95

66. Matsuoka S, Yamamoto K, Ogata T, Kusaba M, Nakashima N, et al. 1993. Efficient and selective electron mediation of cobalt complexes with cyclam and related macrocycles in the p-terphenyl-catalyzed photoreduction of carbon dioxide. *J. Am. Chem. Soc.* 115:601–9
67. Ogata T, Yamamoto Y, Wada Y, Murakoshi K, Kusaba M, et al. 1995. Phenazine-photosensitized reduction of CO₂ mediated by a cobalt-cyclam complex through electron and hydrogen transfer. *J. Phys. Chem.* 99:11916–22
68. Hawecker J, Lehn J-M, Ziessel R. 1983. Efficient photochemical reduction of CO₂ to CO by visible light irradiation of systems containing Re(bipy)(CO)₃X or Ru(bipy)³²⁺-Co²⁺ combinations as homogeneous catalysts. *J. Chem. Soc. Chem. Commun.* 9:536–38
69. Hawecker J, Lehn J-M, Ziessel R. 1986. Photochemical and electrochemical reduction of carbon dioxide to carbon monoxide mediated by (2,2'-bipyridine)tricarbonylchlororhenium(I) and related complexes as homogeneous catalysts. *Helv. Chim. Acta* 69:1990–2012
70. Hori H, Johnson FPA, Koike K, Ishitani O, Ibusuki T. 1996. Efficient photocatalytic CO₂ reduction using [Re(bpy)(CO)₃{P(OEt)₃}]⁺. *J. Photochem. Photobiol. A Chem.* 96:171–74
71. Takeda H, Koike K, Inoue H, Ishitani O. 2008. Development of an efficient photocatalytic system for CO₂ reduction using rhenium(I) complexes based on mechanistic studies. *J. Am. Chem. Soc.* 130:2023–31
72. Gholamkhash B, Mametsuka H, Koike K, Tanabe T, Furue M, Ishitani O. 2005. Architecture of supramolecular metal complexes for photocatalytic CO₂ reduction: ruthenium-rhenium bi- and tetranuclear complexes. *Inorg. Chem.* 44:2326–36
73. Sato S, Koike K, Inoue H, Ishitani O. 2007. Highly efficient supramolecular photocatalysts for CO₂ reduction using visible light. *Photochem. Photobiol. Sci.* 6:454–61
74. Ishida H, Terada T, Tanaka K, Tanaka T. 1990. Photochemical carbon dioxide reduction catalyzed by [Ru(bpy)₂(CO)₂]²⁺ using triethanolamine and 1-benzyl-1,4-dihydronicotinamide as an electron donor. *Inorg. Chem.* 29:905–11
75. Lehn J-M, Ziessel R. 1990. Photochemical reduction of carbon dioxide to formate catalyzed by 2,2'-bipyridine- or 1,10-phenanthroline-ruthenium(II) complexes. *J. Organomet. Chem.* 382:157–73
76. Agarwal J, Johnson RP, Li G. 2011. Reduction of CO₂ on a tricarbonyl rhenium(I) complex: modeling a catalytic cycle. *J. Phys. Chem. A* 115:2877–81
77. Nozik AJ. 1978. Photoelectrochemistry: applications to solar energy conversion. *Annu. Rev. Phys. Chem.* 29:189–222
78. Walter MG, Warren EL, McKone JR, Boettcher SW, Mi Q, et al. 2010. Solar water splitting cells. *Chem. Rev.* 110:6446–73
79. Beley M, Collin JP, Ruppert R, Sauvage JP. 1986. Electrocatalytic reduction of carbon dioxide by nickel cyclam²⁺ in water: study of the factors affecting the efficiency and the selectivity of the process. *J. Am. Chem. Soc.* 108:7461–67
80. Ishida H, Tanaka K, Tanaka T. 1987. Electrochemical CO₂ reduction catalyzed by ruthenium complexes [Ru(bpy)₂(CO)₂]²⁺ and [Ru(bpy)₂(CO)Cl]⁺: effect of pH on the formation of CO and HCOO. *Organometallics* 6:181–86
81. Haines RJ, Wittrig RE, Kubiak CP. 1994. Electrocatalytic reduction of carbon dioxide by the binuclear copper complex [Cu₂(6-(diphenylphosphino-2,2'-bipyridyl)₂(MeCN)₂][PF₆]₂. *Inorg. Chem.* 33:4723–28
82. Kushi Y, Nagao H, Nishioka T, Isobe K, Tanaka K. 1995. Remarkable decrease in overpotential of oxalate formation in electrochemical CO₂ reduction by a metal-sulfide cluster. *J. Chem. Soc. Chem. Commun.* 12:1223–24
83. Tanaka K, Kushi Y, Tsuge K, Toyohara K, Nishioka T, Isobe K. 1998. Catalytic generation of oxalate through a coupling reaction of two CO₂ molecules activated on [(Ir(η⁵-C₅Me₅))₂(Ir(η⁴-C₅Me₅)CH₂CN)(μ₃-S)₂]. *Inorg. Chem.* 37:120–26
84. Rakowski Dubois M, Dubois DL. 2009. Development of molecular electrocatalysts for CO₂ reduction and H₂ production/oxidation. *Acc. Chem. Res.* 42:1974–82
85. DuBois DL, Miedaner A, Haltiwanger RC. 1991. Electrochemical reduction of CO₂ catalyzed by [Pd(triphosphine)(solvent)](BF₄)₂ complexes: synthetic and mechanistic studies. *J. Am. Chem. Soc.* 113:8753–64

86. Morgenstern DA, Wittrig RE, Fanwick PE, Kubiak CP. 1993. Photoreduction of carbon dioxide to its radical anion by nickel cluster $[\text{Ni}_3(\mu_3\text{-I})_2(\text{dppm})_3]$: formation of two carbon-carbon bonds via addition of carbon dioxide radical anion to cyclohexene. *J. Am. Chem. Soc.* 115:6470–71
87. Smieja JM, Kubiak CP. 2010. $\text{Re}(\text{bipy-tBu})(\text{CO})_3\text{Cl}$ -improved catalytic activity for reduction of carbon dioxide: IR-spectroelectrochemical and mechanistic studies. *Inorg. Chem.* 49:9283–89
88. Kumar A, Wilisch WCA, Lewis NS. 1993. The electrical properties of semiconductor/metal, semiconductor/liquid, and semiconductor/conducting polymer contacts. *Crit. Rev. Solid State Mater. Sci.* 18:327–53
89. Bak T, Nowotny J, Rekas M, Sorrell CC. 2002. Photo-electrochemical hydrogen generation from water using solar energy: materials-related aspects. *Int. J. Hydrog. Energy* 27:991–1022
90. Roy SC, Varghese OK, Paulose M, Grimes CA. 2010. Toward solar fuels: photocatalytic conversion of carbon dioxide to hydrocarbons. *ACS Nano* 4:1259–78
91. Hinogami R, Mori T, Yae S, Nakato Y. 1994. Efficient photoelectrochemical reduction of carbon dioxide on a p-type silicon (p-Si) electrode modified with very small copper particles. *Chem. Lett.* 23:1725–28
92. Hinogami R, Nakamura Y, Yae S, Nakato Y. 1997. Modification of semiconductor surface with ultra-fine metal particles for efficient photoelectrochemical reduction of carbon dioxide. *Appl. Surface Sci.* 121/122:301–4
93. Gennaro A, Isse AA, Vianello E. 1990. Solubility and electrochemical determination of CO_2 in some dipolar aprotic solvents. *J. Electroanal. Chem. Interfacial Electrochem.* 289:203–15
94. Taniguchi I. 1989. Electrochemical and photochemical reduction of carbon dioxide. In *Modern Aspects of Electrochemistry*, ed. JO Bockris, RE White, BE Conway, 20:327–400. New York: Plenum
95. Mikkelsen M, Jorgensen M, Krebs FC. 2010. The teraton challenge: a review of fixation and transformation of carbon dioxide. *Energy Environ. Sci.* 3:43–81
96. Tomita Y, Hori Y. 1998. Electrochemical reduction of carbon dioxide at a platinum electrode in acetonitrile-water mixtures. See Ref. 155, pp. 581–84
97. Hara K, Kudo A, Sakata T. 1995. Electrochemical reduction of carbon dioxide under high pressure on various electrodes in an aqueous electrolyte. *J. Electroanal. Chem.* 391:141–47
98. Todoroki M, Hara K, Kudo A, Sakata T. 1995. Electrochemical reduction of high pressure CO_2 at Pb, Hg and In electrodes in an aqueous KHCO_3 solution. *J. Electroanal. Chem.* 394:199–203
99. Hara K, Kudo A, Sakata T, Watanabe M. 1995. High efficiency electrochemical reduction of carbon dioxide under high pressure on a gas diffusion electrode containing Pt catalysts. *J. Electrochem. Soc.* 142:L57–59
100. Hara K, Sakata T. 1997. Electrocatalytic formation of CH_4 from CO_2 on a Pt gas diffusion electrode. *J. Electrochem. Soc.* 144:539–45
101. Sears WM, Morrison SR. 1985. Carbon dioxide reduction on gallium arsenide electrodes. *J. Phys. Chem. A* 89:3295–98
102. Gattrell M, Gupta N, Co A. 2006. A review of the aqueous electrochemical reduction of CO_2 to hydrocarbons at copper. *J. Electroanal. Chem.* 594:1–19
103. Hori Y, Wakebe H, Tsukamoto T, Koga O. 1994. Electrocatalytic process of CO selectivity in electrochemical reduction of CO_2 at metal electrodes in aqueous media. *Electrochim. Acta* 39:1833–39
104. Amatore C, Savéant JM. 1981. Mechanism and kinetic characteristics of the electrochemical reduction of carbon dioxide in media of low proton availability. *J. Am. Chem. Soc.* 103:5021–23
105. Tryk DA, Yamamoto T, Kokubun M, Hirota K, Hashimoto K, et al. 2001. Recent developments in electrochemical and photoelectrochemical CO_2 reduction: involvement of the $(\text{CO}_2)_2$ -dimer radical anion. *Appl. Organometallic Chem.* 15:113–20
106. Jitaru M, Lowy DA, Toma M, Toma BC, Oniciu L. 1997. Electrochemical reduction of carbon dioxide on flat metallic cathodes. *J. Appl. Electrochem.* 27:875–89
107. Peterson AA, Abild-Pedersen F, Studt F, Rossmeisl J, Norskov JK. 2010. How copper catalyzes the electroreduction of carbon dioxide into hydrocarbon fuels. *Energy Environ. Sci.* 3:1311–15
108. Harris LA, Wilson RH. 1978. Semiconductors for photoelectrolysis. *Annu. Rev. Mater. Sci.* 8:99–134
109. Bocarsly AB, Bookbinder DC, Dominey RN, Lewis NS, Wrighton MS. 1980. Photoreduction at illuminated p-type semiconducting silicon photoelectrodes: evidence for Fermi level pinning. *J. Am. Chem. Soc.* 102:3683–88

110. Bard AJ, Bocarsly AB, Fan FRF, Walton EG, Wrighton MS. 1980. The concept of Fermi level pinning at semiconductor/liquid junctions: consequences for energy conversion efficiency and selection of useful solution redox couples in solar devices. *J. Am. Chem. Soc.* 102:3671-77
111. Fan FRF, Bard AJ. 1980. Semiconductor electrodes. 24. Behavior of photoelectrochemical cells based on p-type gallium arsenide in aqueous solutions. *J. Am. Chem. Soc.* 102:3677-83
112. Nagasubramanian G, Wheeler BL, Bard AJ. 1983. Semiconductor electrodes. *J. Electrochem. Soc.* 130:1680-88
113. Bradley MG, Tysak T. 1982. p-Type silicon based photoelectrochemical cells for optical energy conversion: electrochemistry of tetra-azomacrocyclic metal complexes at illuminated. *J. Electroanal. Chem.* 135:153-57
114. Heller A, Miller B, Lewerenz HJ, Bachmann KJ. 1980. An efficient photocathode for semiconductor liquid junction cells: 9.4% solar conversion efficiency with p-InP/VCl₃-VCl₂-HCl/C. *J. Am. Chem. Soc.* 102:6555-56
115. Heller A, Lewerenz HJ, Miller B. 1981. Silicon photocathode behavior in acidic vanadium(II)-vanadium(III) solutions. *J. Am. Chem. Soc.* 103:200-1
116. Soedergrén S, Hagfeldt A, Olsson J, Lindquist S-E. 1994. Theoretical models for the action spectrum and the current-voltage characteristics of microporous semiconductor films in photoelectrochemical cells. *J. Phys. Chem.* 98:5552-56
117. Savéant JM, Vianello E. 1962. Potential-sweep chronoamperometry theory of kinetic currents in the case of a first order chemical reaction preceding the electron-transfer process. *Electrochim. Acta* 8:905-23
118. Bard AJ, Faulkner LR. 2001. *Electrochemical Methods: Fundamentals and Applications*. New York: Wiley
119. Lieber CM, Lewis NS. 1984. Catalytic reduction of carbon dioxide at carbon electrodes modified with cobalt phthalocyanine. *J. Am. Chem. Soc.* 106:5033-34
120. Stalder CJ, Chao S, Wrighton MS. 1984. Electrochemical reduction of aqueous bicarbonate to formate with high current efficiency near the thermodynamic potential at chemically derivatized electrodes. *J. Am. Chem. Soc.* 106:3673-75
121. O'Toole TR, Margerum LD, Westmoreland TD, Vining WJ, Murray RW, Meyer TJ. 1985. Electrocatalytic reduction of CO₂ at a chemically modified electrode. *J. Chem. Soc. Chem. Commun.* 20:1416-17
122. Cosnier S, Deronzier A, Moutet J-C. 1988. Electrocatalytic reduction of CO₂ on electrodes modified by fac-Re(2,2'-bipyridine)(CO)₃Cl complexes bonded to polypyrrole films. *J. Mol. Catalysis* 45:381-91
123. O'Toole TR, Sullivan BP, Bruce MRM, Margerum LD, Murray RW, Meyer TJ. 1989. Electrocatalytic reduction of CO₂ by a complex of rhenium in thin polymeric films. *J. Electroanal. Chem.* 259:217-39
124. Chardon-Noblat S, Collomb-Dunand-Sauthier MN, Deronzier A, Ziessel R, Zsoldos D. 1994. Formation of polymeric [{Ru⁰(bpy)(CO)₂}]_n films by electrochemical reduction of [Ru(bpy)₂(CO)₂](PF₆)₂: its implication in CO₂ electrocatalytic reduction. *Inorg. Chem.* 33:4410-12
125. Collomb-Dunand-Sauthier M-N, Deronzier A, Ziessel R. 1994. Electrocatalytic reduction of carbon dioxide with mono(bipyridine)carbonylruthenium complexes in solution or as polymeric thin films. *Inorg. Chem.* 33:2961-67
126. Ramos Sende JA, Arana CR, Hernandez L, Potts KT, Keshevarz-K M, Abruna HD. 1995. Electrocatalysis of CO₂ reduction in aqueous media at electrodes modified with electropolymerized films of vinylterpyridine complexes of transition metals. *Inorg. Chem.* 34:3339-48
127. Chardon-Noblat S, Deronzier A, Ziessel R, Zsoldos D. 1998. Electroreduction of CO₂ catalyzed by polymeric [Ru(bpy)(CO)₂]_n films in aqueous media: parameters influencing the reaction selectivity. *J. Electroanal. Chem.* 444:253-60
128. Ziessel R. 1998. Molecular tailoring of organometallic polymers for efficient catalytic CO₂ reduction: mode of formation of the active species. See Ref. 155, pp. 219-24
129. Cecchet F, Alebbi M, Bignozzi CA, Paolucci F. 2006. Efficiency enhancement of the electrocatalytic reduction of CO₂: fac-[Re(v-bpy)(CO)₃Cl] electropolymerized onto mesoporous TiO₂ electrodes. *Inorg. Chim. Acta* 359:3871-74
130. Parkin A, Seravalli J, Vincent KA, Ragsdale SW, Armstrong FA. 2007. Rapid and efficient electrocatalytic CO₂/CO interconversions by carboxydotherrmus hydrogenofomans CO dehydrogenase I on an electrode. *J. Am. Chem. Soc.* 129:10328-29

131. Cheung K-C, Guo P, So M-H, Lee LYS, Ho K-P, et al. 2009. Electrocatalytic reduction of carbon dioxide by a polymeric film of rhenium tricarbonyl dipyridylamine. *J. Organomet. Chem.* 694:2842-45
132. Smith RDL, Pickup PG. 2010. Nitrogen-rich polymers for the electrocatalytic reduction of CO₂. *Electrochem. Commun.* 12:1749-51
133. Collin JP, Sauvage JP. 1989. Electrochemical reduction of carbon dioxide mediated by molecular catalysts. *Coord. Chem. Rev.* 93:245-68
134. Abe T, Kaneko M. 2003. Reduction catalysis by metal complexes confined in a polymer matrix. *Prog. Polym. Sci.* 28:1441-88
135. Abe T, Yoshida T, Tokita S, Taguchi F, Imaiya H, Kaneko M. 1996. Factors affecting selective electrocatalytic CO₂ reduction with cobalt phthalocyanine incorporated in a polyvinylpyridine membrane coated on a graphite electrode. *J. Electroanal. Chem.* 412:125-32
136. Chen Z, Concepcion JJ, Jurss JW, Meyer TJ. 2009. Single-site, catalytic water oxidation on oxide surfaces. *J. Am. Chem. Soc.* 131:15580-81
137. Yoshida T, Tsutsumida K, Teratani S, Yasufuku K, Kaneko M. 1993. Electrocatalytic reduction of CO₂ in water by [Re(bpy)(CO)₃Br] and [Re(terpy)(CO)₃Br] complexes incorporated into coated nafion membrane (bpy = 2,2'-bipyridine; terpy = 2,2';6',2''-terpyridine). *J. Chem. Soc. Chem. Commun.* 7:631-33
138. Dominey RN, Lewis NS, Bruce JA, Bookbinder DC, Wrighton MS. 1982. Improvement of photoelectrochemical hydrogen generation by surface modification of p-type silicon semiconductor photocathodes. *J. Am. Chem. Soc.* 104:467-82
139. Wrighton MS. 1983. Chemically derivatized semiconductor photoelectrodes. *J. Chem. Educ.* 60:335-37
140. Wrighton MS. 1986. Surface functionalization of electrodes with molecular reagents. *Science* 231:32-37
141. Lewis NS. 2005. Chemical control of charge transfer and recombination at semiconductor photoelectrode surfaces. *Inorg. Chem.* 44:6900-11
142. Kumar A, Wilisch WCA, Lewis NS. 1993. The electrical properties of semiconductor/metal, semiconductor/liquid, and semiconductor/conducting polymer contacts. *Crit. Rev. Solid State Mater. Sci.* 18:327-53
143. Huang J, Stockwell D, Huang Z, Mohler DL, Lian T. 2008. Photoinduced ultrafast electron transfer from CdSe quantum dots to re-bipyridyl complexes. *J. Am. Chem. Soc.* 130:5632-33
144. Sato S, Morikawa T, Saeiki S, Kajino T, Motohiro T. 2010. Visible-light-induced selective CO₂ reduction utilizing a ruthenium complex electrocatalyst linked to a p-type nitrogen-doped Ta₂O₅ semiconductor. *Angew. Chem. Int. Ed.* 49:5101-5
145. Woolerton TW, Sheard S, Reisner E, Pierce E, Ragsdale SW, Armstrong FA. 2010. Efficient and clean photoreduction of CO₂ to CO by enzyme-modified TiO₂ nanoparticles using visible light. *J. Am. Chem. Soc.* 132:2132-33
146. Anuso CL, Snoberger RC, Ricks AM, Liu W, Xiao D, et al. 2011. Covalent attachment of a rhenium bipyridyl CO₂ reduction catalyst to rutile TiO₂. *J. Am. Chem. Soc.* 133:6922-25
147. Licht S, Wang B, Mukerji S, Soga T, Umeno M, Tributsch H. 2000. Efficient solar water splitting, exemplified by RuO₂-catalyzed AlGaAs/Si photoelectrolysis. *J. Phys. Chem. B* 104:8920-24
148. Khaselev O, Bansal A, Turner JA. 2001. High-efficiency integrated multijunction photovoltaic/electrolysis systems for hydrogen production. *Int. J. Hydrog. Energy* 26:127-32
149. Yamada Y, Matsuki N, Ohmori T, Mametsuka H, Kondo M, et al. 2003. One chip photovoltaic water electrolysis device. *Int. J. Hydrog. Energy* 28:1167-69
150. Yamane S, Kato N, Kojima S, Imanishi A, Ogawa S, et al. 2009. Efficient solar water splitting with a composite n-Si/p-CuI/n-i-p a-Si/n-p GaP/RuO₂ semiconductor electrode. *J. Phys. Chem. C* 113:14575-81
151. Dang T, Ramsaran R, Roy S, Froehlich J, Wang J, Kubiak C. 2011. Design of a high throughput 25-well parallel electrolyzer for the accelerated discovery of CO₂ reduction catalysts via a combinatorial approach. *Electroanalysis* 23:2335-42
152. Ellis WW, Raebiger JW, Curtis CJ, Bruno JW, DuBois DL. 2004. Hydricities of BzNADH, C₅H₅Mo(PMe₃)(CO)(2)H, and C₅Me₅Mo(PMe₃)(CO)(2)H in acetonitrile. *J. Am. Chem. Soc.* 126:2738-43

153. Zhu XQ, Tan Y, Cao CT. 2010. Thermodynamic diagnosis of the properties and mechanism of dihydropyridine-type compounds as hydride source in acetonitrile with “molecule ID card.” *J. Phys. Chem. B* 114:2058–75
154. Creutz C, Chou MH. 2009. Hydricities of d(6) metal hydride complexes in water. *J. Am. Chem. Soc.* 131:2794–95
155. Inui T, Anpo M, Izui K, Yanagida S, Yamaguchi T, eds. 1998. *Studies in Surface Science and Catalysis*, Vol. 114. Amsterdam: Elsevier



Contents

Membrane Protein Structure and Dynamics from NMR Spectroscopy <i>Mei Hong, Yuan Zhang, and Fanghao Hu</i>	1
The Polymer/Colloid Duality of Microgel Suspensions <i>L. Andrew Lyon and Alberto Fernandez-Nieves</i>	25
Relativistic Effects in Chemistry: More Common Than You Thought <i>Pekka Pyykkö</i>	45
Single-Molecule Surface-Enhanced Raman Spectroscopy <i>Eric C. Le Ru and Pablo G. Etchegoin</i>	65
Singlet Nuclear Magnetic Resonance <i>Malcolm H. Levitt</i>	89
Environmental Chemistry at Vapor/Water Interfaces: Insights from Vibrational Sum Frequency Generation Spectroscopy <i>Aaron M. Jubb, Wei Hua, and Heather C. Allen</i>	107
Extensivity of Energy and Electronic and Vibrational Structure Methods for Crystals <i>So Hirata, Murat Keçeli, Yu-ya Ohnishi, Olaseni Sode, and Kiyoshi Yagi</i>	131
The Physical Chemistry of Mass-Independent Isotope Effects and Their Observation in Nature <i>Mark H. Thiemens, Subrata Chakraborty, and Gerardo Dominguez</i>	155
Computational Studies of Pressure, Temperature, and Surface Effects on the Structure and Thermodynamics of Confined Water <i>N. Giovambattista, P.J. Rossky, and P.G. Debenedetti</i>	179
Orthogonal Intermolecular Interactions of CO Molecules on a One-Dimensional Substrate <i>Min Feng, Chungwei Lin, Jin Zhao, and Hrvoje Petek</i>	201
Visualizing Cell Architecture and Molecular Location Using Soft X-Ray Tomography and Correlated Cryo-Light Microscopy <i>Gerry McDermott, Mark A. Le Gros, and Carolyn A. Larabell</i>	225

Deterministic Assembly of Functional Nanostructures Using Nonuniform Electric Fields <i>Benjamin D. Smith, Theresa S. Mayer, and Christine D. Keating</i>	241
Model Catalysts: Simulating the Complexities of Heterogeneous Catalysts <i>Feng Gao and D. Wayne Goodman</i>	265
Progress in Time-Dependent Density-Functional Theory <i>M.E. Casida and M. Huix-Rotllant</i>	287
Role of Conical Intersections in Molecular Spectroscopy and Photoinduced Chemical Dynamics <i>Wolfgang Domcke and David R. Yarkony</i>	325
Nonlinear Light Scattering and Spectroscopy of Particles and Droplets in Liquids <i>Sylvie Roke and Grazia Gonella</i>	353
Tip-Enhanced Raman Spectroscopy: Near-Fields Acting on a Few Molecules <i>Bruno Pettinger, Philip Schambach, Carlos J. Villagómez, and Nicola Scott</i>	379
Progress in Modeling of Ion Effects at the Vapor/Water Interface <i>Roland R. Netz and Dominik Horinek</i>	401
DEER Distance Measurements on Proteins <i>Gunnar Jeschke</i>	419
Attosecond Science: Recent Highlights and Future Trends <i>Lukas Gallmann, Claudio Cirelli, and Ursula Keller</i>	447
Chemistry and Composition of Atmospheric Aerosol Particles <i>Charles E. Kolb and Douglas R. Worsnop</i>	471
Advanced Nanoemulsions <i>Michael M. Fryd and Thomas G. Mason</i>	493
Live-Cell Super-Resolution Imaging with Synthetic Fluorophores <i>Sebastian van de Linde, Mike Heilemann, and Markus Sauer</i>	519
Photochemical and Photoelectrochemical Reduction of CO ₂ <i>Bhupendra Kumar, Mark Llorente, Jesse Froeblich, Tram Dang, Aaron Sathrum, and Clifford P. Kubiak</i>	541
Neurotrophin Signaling via Long-Distance Axonal Transport <i>Praveen D. Chowdary, Dung L. Che, and Bianxiao Cui</i>	571
Photophysics of Fluorescent Probes for Single-Molecule Biophysics and Super-Resolution Imaging <i>Taekjip Ha and Philip Tinnefeld</i>	595

Ultrathin Oxide Films on Metal Supports: Structure-Reactivity Relations <i>S. Shaikbutdinov and H.-J. Freund</i>	619
Free-Electron Lasers: New Avenues in Molecular Physics and Photochemistry <i>Joachim Ullrich, Artem Rudenko, and Robert Moshammer</i>	635
Dipolar Recoupling in Magic Angle Spinning Solid-State Nuclear Magnetic Resonance <i>Gaël De Paëpe</i>	661

Indexes

Cumulative Index of Contributing Authors, Volumes 59–63	685
Cumulative Index of Chapter Titles, Volumes 59–63	688

Errata

An online log of corrections to Annual Review of Physical Chemistry chapters (if any, 1997 to the present) may be found at <http://physchem.AnnualReviews.org/errata.shtml>